Rivista Italiana di Paleontologia e Stratigrafia
(*Research in Paleontology and Stratigraphy*)
vol. 125(1): 147-181. **March 2019**

LOWER TRIASSIC (INDUAN TO OLENEKIAN) CONODONTS, FORAMINIFERA AND BIVALVES FROM THE AL MAMALIH AREA, DEAD SEA, JORDAN: CONSTRAINTS ON THE P-T BOUNDARY

JOHN H. POWELL[1*], ALDA NICORA[2], MARIA CRISTINA PERRI[3], ROBERTO RETTORI[4], RENATO POSENATO[5], MICHAEL H. STEPHENSON[1], AHMED MASRI[6], LETIZIA M. BORLENGHI[2] & VALERIO GENNARI[4]

[1*]Corresponding author. British Geological Survey, Nottingham NG12 5GG, UK. E-mail: jhp@bgs.ac.uk; mhste@bgs.ac.uk
[2]Dipartimento di Scienze della Terra "A. Desio", Via Mangiagalli 34, 20133 Milano, Italy. E-mail: alda.nicora@unimi.it
[3]Dipartimento di Scienze Biologiche, Geologiche e Ambientali, Via Zamboni 67, 40136 Bologna, Italy. E-mail: mariacristina.perri@unibo.it
[4]Dipartimento di Fisica e Geologia, Via Alesssandro Pascoli, 06123, Perugia, Italy. E-mail: roberto.rettori@unipg.it
[5]Dipartimento di Fisica e Scienze della Terra, Università di Ferrara, Via Saragat 1, 44121 Ferrara, Italy. E-mail: psr@unife.it
[6]Ministry of Energy and Mineral Resources (MEMR), Geological Mapping Division, Amman, Jordan. E-mail: aiamsri@yahoo.com

To cite this article: Powell J.H., Nicora A., Perri M.C., Rettori R., Posenato R., Stephenson M.H., Masri A., Borlenghi L.M. & Gennari V. (2019) - Lower Triassic (Induan to Olenekian) conodonts, foraminifera and bivalves from the Al Mamalih area, Dead Sea, Jordan: constraints on the P-T boundary. *Riv. It. Paleontol. Strat.*, 125(1): 147-181.

Keywords: Permian-Triassic succession; conodonts; foraminifera; bivalves; Jordan.

Abstract. Upper Permian to Lower Triassic successions exposed in the Al Mamalih area, east of the Dead Sea, Jordan record the transition between the alluvial Umm Irna Formation (Upper Permian) and the overlying shallow marine Ma'in Formation (Lower Triassic). The Permian-Triassic boundary is constrained either within a hiatus represented by a sequence boundary between these formations or within ca 15 m of shallow marine beds overlying the boundary. Above the sequence boundary reddened, shallow-marine beds (Himara Member) mark the initial Triassic (presumed early Induan) marine transgression (Himara Member). Absence of both body fossils and vertical infaunal burrows indicates low-diversity ecosystems following the Permian-Triassic extinction event. A gradational upward increase in grey, green and yellow siltstones beds (Nimra Member), accompanied by a concomitant increase in bioturbation (surface traces and infaunal vertical burrows), bivalves and brachiopods, stromatolites, conchostracans and lingulids in the lower part of the Nimra Member indicates colonisation of the substrate under shallow marine conditions during the recovery phase. Shallow-water carbonates in the Nimra Member yielded an abundant, low diversity assemblage of conodonts (e.g. *Hd. aequabilis* and *H. agordina*) and a foraminifera assemblage (*Postcladella* gr. *kalhori-Earlandia* spp.-*Ammodiscus jordanensis* n. sp.) that are interpreted as euryhaline recovery taxa that characterise the mid-late Induan. Abundant new material has allowed revision of the conodont apparatus and the foraminifera include a new species *Ammodiscus jordanensis* n. sp. of Induan age. The discovery of the bivalves *Claraia bittneri* (*C. aurita* group) and *Eumorphotis multiformis* is worthy of note. Upper Permian alluvial lithofacies (Jordan) pass basinwards, about 50 km to the northwest, to coeval shallow marine siliciclastic and carbonates in the Negev and Mediterranean coast of Israel.

Introduction

The transitional Upper Permian to Lower Triassic succession (Figs 1 and 2) outcrops along the margins of the Dead Sea, Jordan (Cox 1924, 1932; Huckriede & Stoppel (in Bender 1974); Bandel & Khoury 1981; Makhlouf et al. 1991) and has been described in detail in recent papers (Abu Hamad et al. 2008; Stephenson & Powell 2013, 2014; Powell et al. 2016). The succession spans the Late Permian to Early Triassic, the lower age of which has been constrained, in Jordan, by plant macrofossils (Abu Hamad et al. 2008) and palynomorphs (Stephenson & Powell 2013, 2014) in strata interpreted to be of alluvial origin (Umm Irna Formation), and by sparse conodonts, foraminifera and conchostracans (Scholze et al. 2015; Powell et al. 2016) from overlying Lower Triassic rocks of shallow marine origin (Ma'in Formation).

Received: August 29, 2018; accepted: February 13, 2019

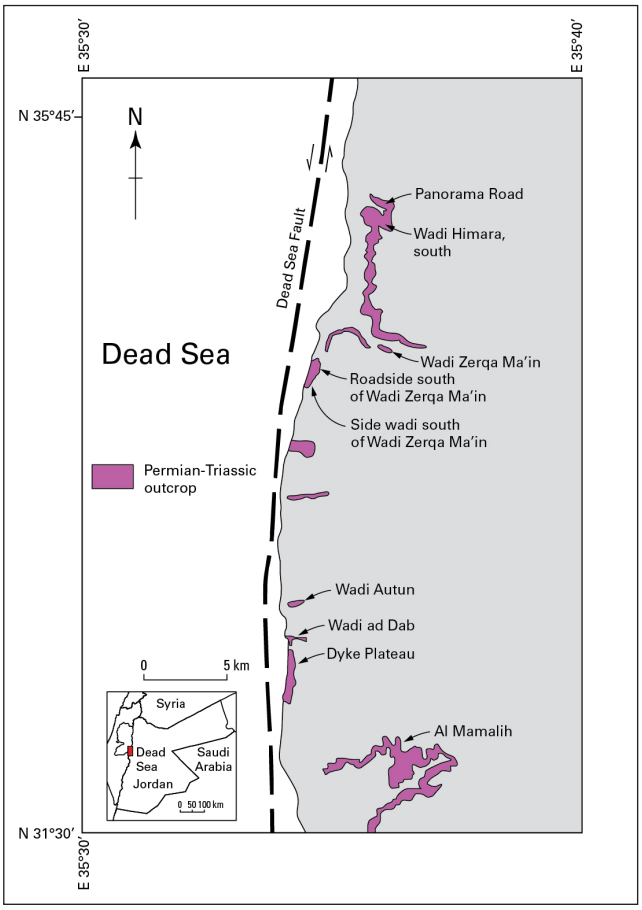

Fig. 1 - Location of the outcrop of the Upper Permian to Lower Triassic Umm Irna and Ma'in formations at Al Mamalih, and the sections along the Dead Sea margins including the Dyke Plateau locality (after Powell et al. 2016).

Stephenson & Powell (2013) related the sedimentary sequences and alluvial architecture in the Umm Irna Formation to major sequence-stratigraphical events (depositional sequences) during the Middle to Late Permian (Wordian to Wuchiapingian) across the Arabian Plate, located in the equatorial zone at the southern margin of the Neo-Tethys Ocean (Stamplfi & Borel 2002). The top of the alluvial Umm Irna Formation is a major sequence boundary (Stephenson & Powell 2013, fig. 7), and is overlain by red-bed shallow-marine siliciclastic rocks (Himara Member, Ma'in Formation) passing up to greenish-grey-yellow marine siliciclastic rocks and thin carbonates (Nimra Member) (Powell et al. 2016). Thin limestone (wacke-packstone) beds with shallow scours and bivalve shell lags, yielded a low diversity assemblage of conodonts (e.g. *Hadrodontina aequabilis*) and foraminifera (e.g. "*Cornuspira*" *mahajeri*) that were interpreted as euryhaline taxa characterising the Induan (Powell et al. 2016).

In this paper we describe new sections across the P-T boundary located in the Al Mamalih area, located inland about 7 km to the south-east of the Dead Sea coastal outcrops described earlier. The P-T succession in the Al Mamalih area was first described by Powell & Moh'd (1993), who recognised the importance of the localities at the southernmost outcrop (shoreline margins) of the Permian-Triassic succession in Jordan. We describe conodonts, foraminifera, including a new species (*Ammodiscus jordanensis* n. sp.), and bivalves (including *Claraia*) from thin calcareous sandstones and sandy limestones in the Lower Triassic Nimra Member and from the stratigraphically higher Upper Carbonate Member of the Dardun Formation.

Geological setting

In Jordan, the Permian to Triassic succession sequence thins southward along the Dead Sea shore below the overstepping, unconformable Lower Cretaceous Kurnub Sandstone (Wetzel & Morton 1959; Bender 1974; Moh'd 1989; Powell & Moh'd 1993; Shawabakeh 1998), wedging out just south of the Al Mamalih area (Fig. 1). To the north of Wadi Zarqa Ma'in, the Permian, Triassic and Jurassic succession is more complete and is preserved below the Lower Cretaceous (Kurnub) unconformity (Bandel & Khoury 1981; Powell & Moh'd 1993) reflecting the relative completeness of the Lower Permian to Jurassic succession in north Jordan, as compared to the Dead Sea and Al Mamalih area (this study). This is due to step-like, northerly extensional down-faulting of the succession in pre-Cretaceous (Kurnub) times, probably during the Late Jurassic (Powell & Moh'd 1993).

The Middle to Upper Permian Umm Irna Formation, unconformably overlies Cambrian sandstones (Umm Ishrin Sandstone Formation; Powell 1989; Powell et al. 2014) and, in turn, is overlain by the Lower Triassic succession comprising, in upward sequence, the Himara and Nimra members of the Ma'in Formation and the Dardun Formation (Bandel & Khoury 1981; Makhlouf 1987) (Figs 1, 2 and 3). In the Al Mamalih area, the uppermost Umm Irna Formation and the Himara/Nimra members (Figs 3 and 4) are exposed in a series of narrow horsts and grabens that were formed during a Late Jurassic extensional tectonic episode prior to

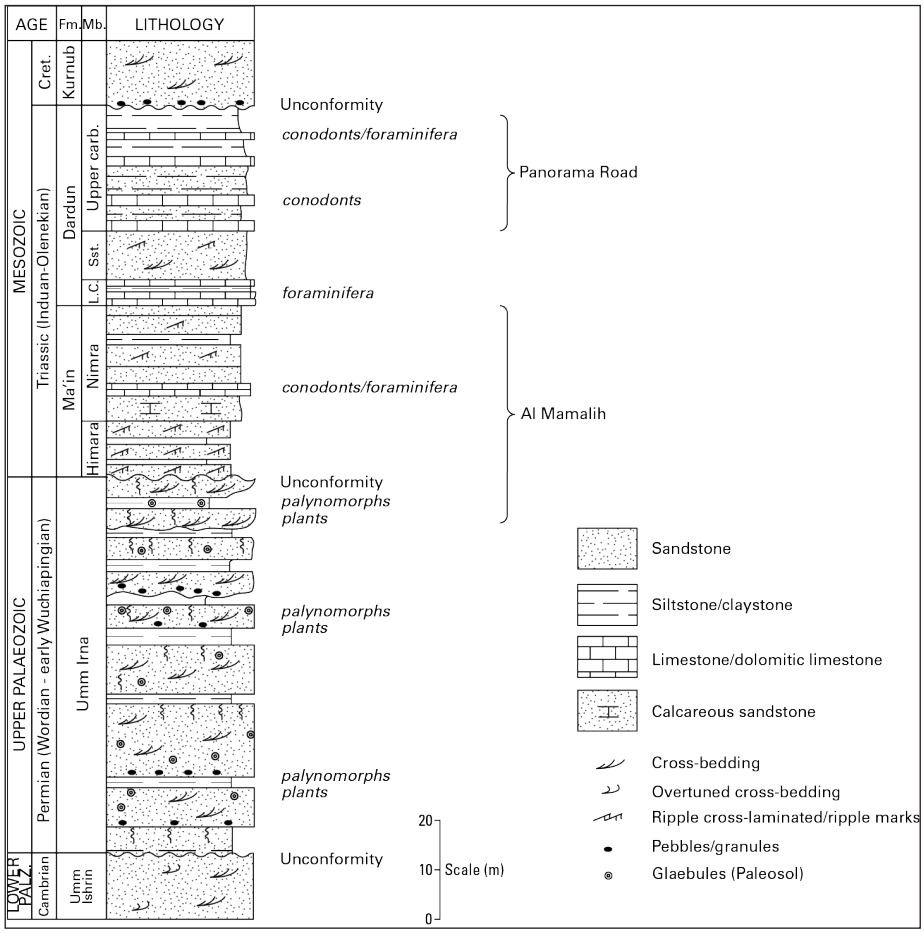

Fig. 2 - Generalised Permian to Lower Triassic succession in the study area (after Bandel & Khoury 1981). The position of the Al Mamalih and Dyke Plateau locality sections is shown.

deposition of the overstepping Lower Cretaceous Kurnub Sandstone (Powell & Moh'd 1993).

West of the Dead Sea but offset by a ca 110 km left-lateral shear on the Neogene Dead Sea Transform (Freund et al. 1970), Permian sediments were deposited in a shallow marine environment with inter-fingering fluvial siliciclastics representing the paleoshoreline in the Negev area (Eshet & Cousminer 1986; Eshet 1990; Hirsch 1975; Korngreen & Zilberman 2017). Farther west, i.e. basinwards, near the present-day coastline of Israel the P-T succession is wholly marine in character (Korngreen et al. 2013).

Paleogeographic reconstructions for the Permian-Triassic interval in the Levant indicate that the region lay about 15 to 20 degrees south of the paleo-equator at the northern margin of the Arabian Platform in a continental to shallow marine setting with the Neo-Tethys Ocean located to the north (Stampfli & Borel 2002; Powell et al. 2016, fig. 4). During high relative sea-level stands, marine transgressions advanced to the south and south east (Alsharhan & Nairn 1997) across the regional Hail-Rutbah Arch in the subsurface of eastern Jordan and Saudi Arabia (Sharland et al. 2001, 2004). The paleogeographical location, together with diverse and prolific macro- and micro-floras from the uppermost Umm Irna Formation (early Wuchiapingian), and the presence of ferralitic paleosols, indicate deposition in a humid-tropical climate (Makhlouf 1987; Makhlouf et al. 1991; Kerp et al. 2006; Stephenson & Powell 2013). Shallow-water siliciclastics with thin carbonate beds were deposited in warm seas at the southeast margin of the basin during the Early Triassic (Induan) transgression (Powell et al. 2016).

Materials and Methods

Measured sections (Fig. 1) were logged at 4 localities (Figs 3 to 4) within faulted horst and graben sections in the Al Mamalih area that expose the Umm Irna and Ma'in formations (Figs 7 to 10). As noted above, the upper parts of the Lower Triassic Nimra Member are absent due to the overstepping Lower Cretaceous (Kurnub) unconformity. In addition, the carbonate-rich beds in the Dyke Plateau sections (Cliff/Track Section and Roadside Section, Figs 5, 11a) described by Powell et al. (2016) were re-sampled (Sample numbers AN 2-14) for additional conodont/foraminifera faunas. A fourth section was studied adjacent to the Panorama Road (Figs 6, 11b) which comprises the stratigraphically higher Dardun Formation.

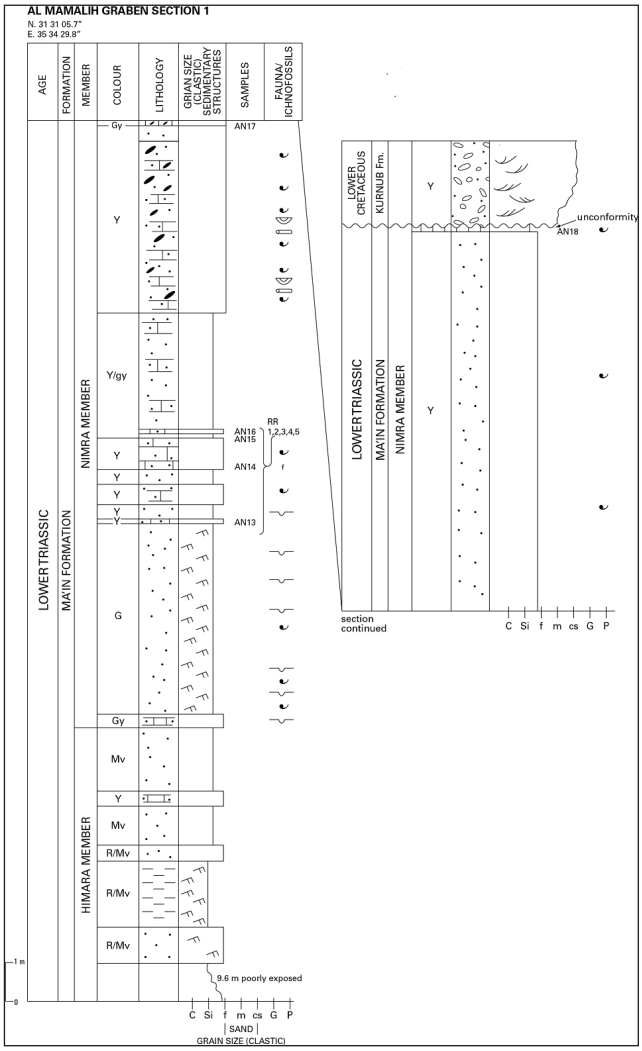

Fig. 3 - Graphic log of the Lower Triassic Al Mamalih graben Section 1. N. 31 31 05.7; E 35 34 29.8. See Fig. 5 for Key. AN and RR indicate sample numbers.

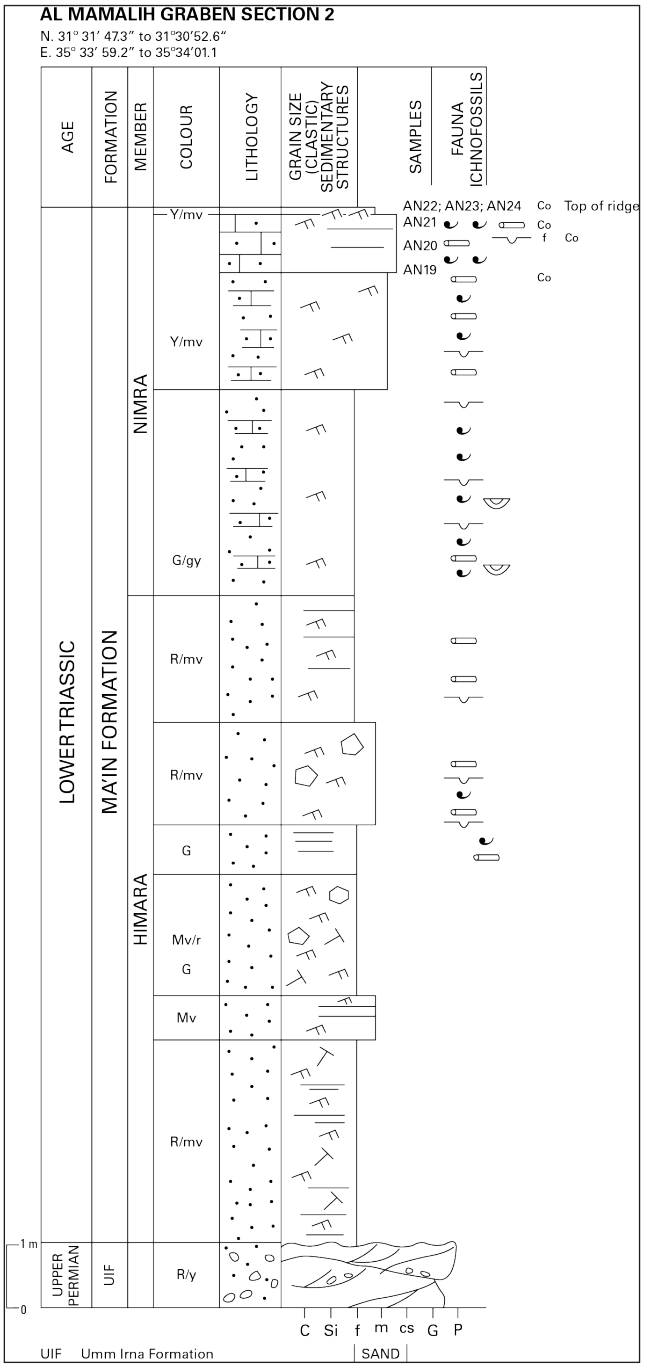

Fig. 4 - Graphic log of the Upper Permian and Lower Triassic Al Mamalih graben Section 2. N. 31 31 47.3; E 35 33 59.2 to N. 31 30 52.6 E. 35 34 01.1. See Fig. 5 for Key. AN indicates sample numbers.

Localities were recorded with a high-resolution digital camera and GPS. Thirty-six samples of limestone and sandy limestone were collected for conodont and foraminiferal analysis from the Nimra Member (Ma'in Formation) and the Upper Carbonate Member (Dardun Formation). Stained petrological thin sections of the limestones were produced for foraminiferal and microfacies analysis. Conodonts were extracted by acid leaching in 10% formic acid. Complete and broken conodont elements were picked from the >125-micron fraction of the acid-insoluble residues.

Lithostratigraphy and sedimentology of the Al Mamalih sections

Previous studies of the Umm Irna Formation (Bandel & Khoury 1981; Makhlouf 1987; Makhlouf et al. 1991; Powell & Moh'd 1993; Dill et al. 2010; Stephenson & Powell 2013) demonstrated depositional environments typified by predominantly fluvial, low-sinuosity and meandering sandstone channels, the latter more common in the upper part, together with epsilon cross-stratification with claystones preserving a diverse and abundant macro-plant assemblage (Abu Hamad 2008). Interfluve sediments comprise finer grained, red-bed sandstone, siltstone and claystone with intermittent ferruginous palaeosol horizons. Organic-rich mudstones and thin im-

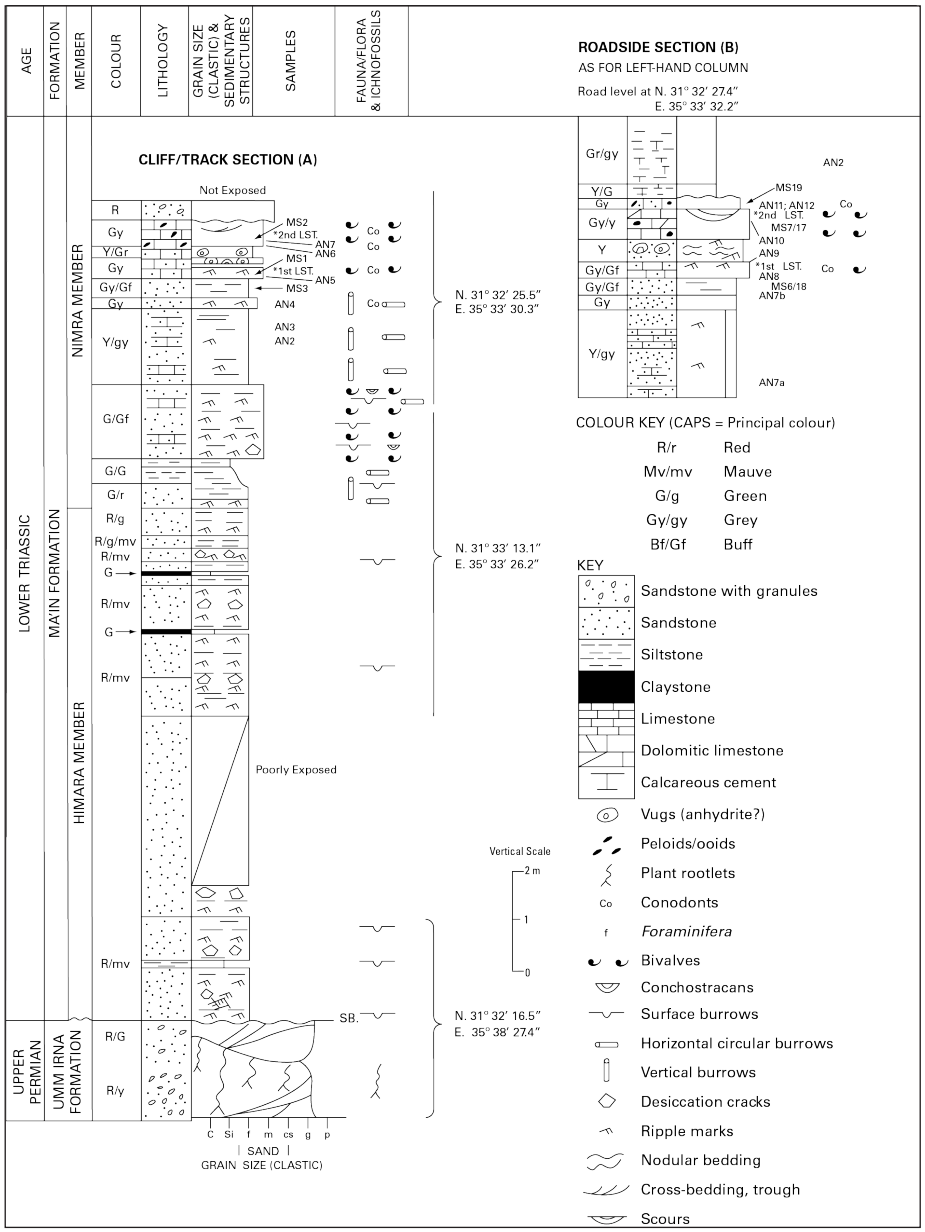

Fig. 5 - Graphic log of the Upper Permian to Lower Triassic succession in the Dyke Plateau and Roadside sections (after Powell et al. 2016). Roadside section B is located 200 m east of the Cliff/track section A. SB is the sequence boundary between the Umm Irna and Ma'in formations. MS and AN (this study) indicate sample numbers.

mature coals (some with seatearths) are occasionally present. The overlying Triassic Ma'in Formation (Figs 3, 4) comprises red and green (often mottled) claystone, siltstone and fine-grained sandstone (Himara Member), passing up to green, grey, buff and yellow fine-grained sandstone with thin, cross-bedded wackestone – packstone beds.

The principal lithofacies of the Al Mamalih sections are summarized below (Localities 1 and 2). Details of the Dyke Plateau sections are given in Powell et al. (2016), but because the Roadside Section (Locality 3) was extended downwards and re-sampled for fauna (Samples AN 2-12 herein) it is reproduced here with additions. The Panorama Road section (Fig. 6) exposes the Lower Carbonate Member of the overlying Dardun Formation (Bandel & Khoury 1981).

Section 1, Al Mamalih; Ma'in Formation; Himara Member and Nimra Members

This section (Figs 3, 7), spans the Himara and Nimra members of the Ma'in Formation; the base of the Himara Member is poorly exposed but is interpreted, by comparison with Section 2, to lie about 4 m below the base of the section.

The Himara Member (up to 6 m thick) consists of alternating red and mauve siltstone and fine-grained sandstone beds with ripple cross-lamination and desiccation cracks. Trace fossils and body fossils are sparse.

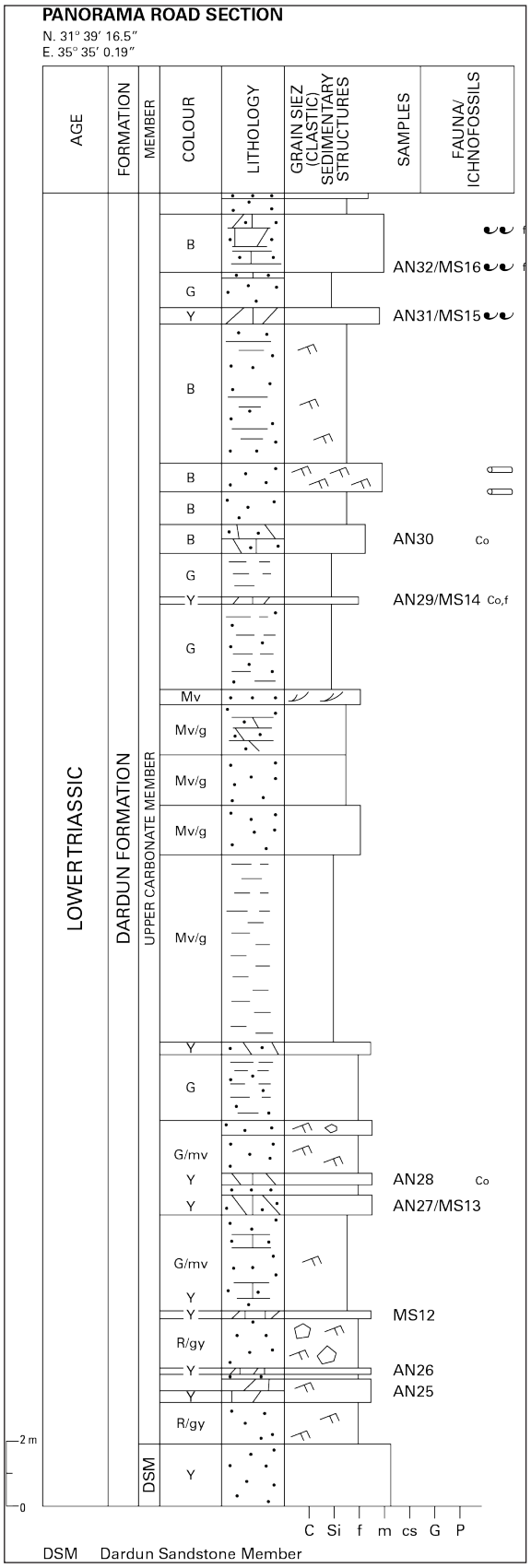

Fig. 6 - Graphic log of the lower part of the Lower Triassic Dardun Formation exposed near the Panorama Road at N. 31 39 16.5; E 36 35 0.19. DSM = Dardun Sandstone Member. AN and MS indicate sample numbers.

The boundary with the Nimra Member is marked by a colour change to grey, green and yellow, fine-grained calcareous, glauconitic sandstone with ripple cross-lamination, indeterminate surface burrow traces, along with poorly preserved thin-shelled decalcified bivalves and possible conchostracans in the lower 5 m. Above this, yellow and grey colours reflect increasingly carbonate-rich cements in the fine-grained calcareous sandstones interbedded with partly dolomitized (and recrystalized) packstone with fragments of bivalves, crinoids, gastropods and brachiopods; glauconite and phosphate peloids are also present. Bedding plane surfaces reveal poorly preserved bivalves, conchostracans, and abundant surface burrows. Sparse foraminifera include a new species *Ammodiscus jordanensis* n. sp. (see below). The pebbly, coarse-grained Lower Cretaceous Kurnub Sandstone rests unconformably above. Samples AN 13 to AN 18 were collected from the carbonate-rich beds.

Section 2, Al Mamalih; Umm Irna Formation; Ma'in Formation, Himara and Nimra members

This section includes the sequence boundary with the underlying Umm Irna Formation and terminates at the top of a ridge within the Nimra Member (Figs 4, 8); the unconformable Kurnub Sandstone is absent due to erosion. The uppermost 1 m of the Umm Irna Formation is shown in Fig. 8, but the section extends downwards to include the lower unconformable boundary with the Cambrian Umm Ishrin Sandstone (Powell & Moh'd 1993; Powell et al. 2014). Umm Irna Formation lithofacies are similar to those reported from the Dead Sea coastal exposures (Stephenson & Powell 2013) comprising stacked channel sandstones, mostly with granule to coarse-grained, cross-bedded sandstone fill, and overbank sandstones with ferruginous paleosols. However, in contrast to the Dead Sea sections, no fine-grained claystones with plant-rich organic material were seen. This suggests higher fluvial channel velocities in the Al Mamalih area and an absence of meandering channels where plants might be preserved during waning flow.

The lowermost Himara Member comprises red-mauve, fine-grained sandstone with ripple marks and ripple cross-lamination (Fig. 9), and parallel laminated beds with syneresis cracks and desiccation cracks (Fig. 9) on bedding planes. An

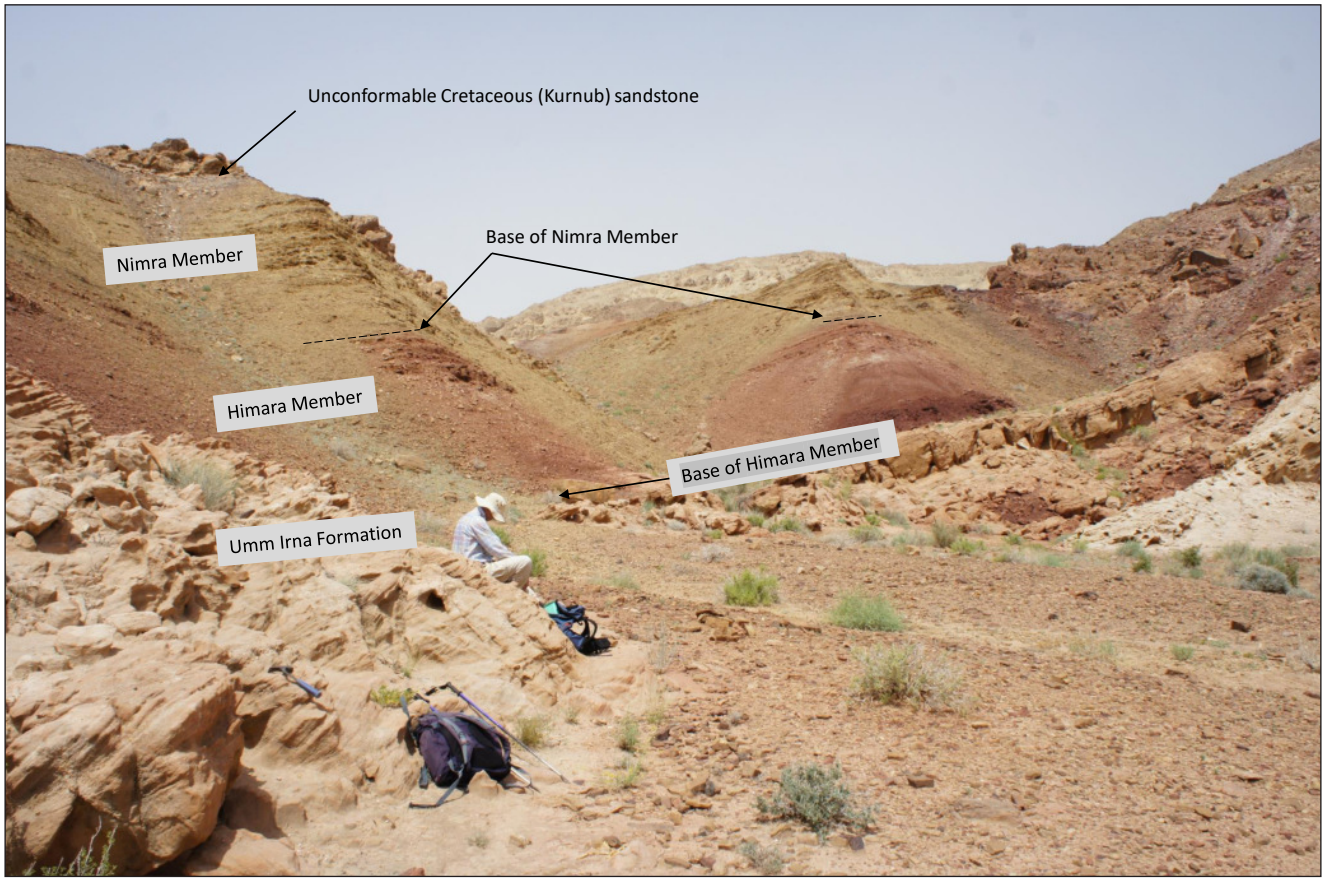

Fig. 7 - Al Mamalih section 1, showing the Upper Permian Umm Irna Fm. fluvial sandstone in the foreground and small ridge dipping to the left; red siltstone and fine-grained sandstone of the Himara Member overlain by green-grey calcareous siltstone and sandy limestone of the Nimra Member and the unconformable Cretaceous Kurnub Sandstone above. See Fig. 3 for detailed log.

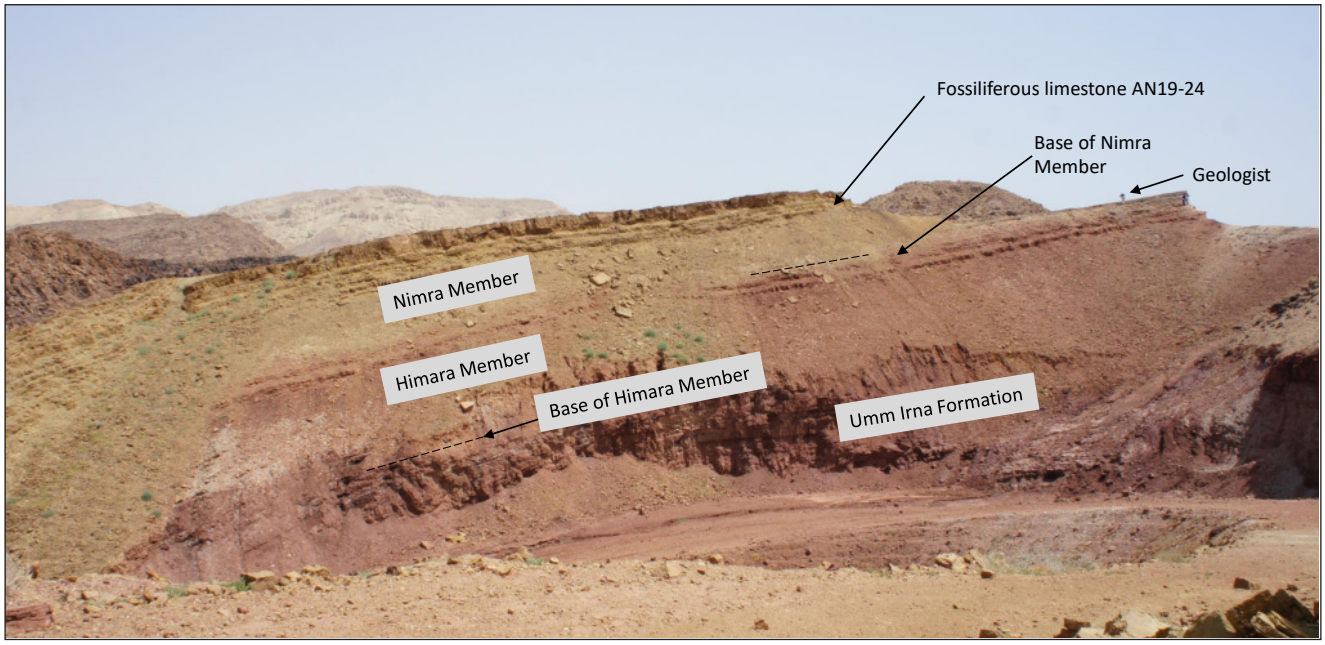

Fig. 8 - Al Mamalih section 2, showing the Upper Permian Umm Irna Fm. fluvial sandstone (red beds) at the base, red siltstones and fine-grained sandstone of the Himara Member overlain by green-grey calcareous siltstone and sandy limestone of the Nimra Member. The fossiliferous sandy limestone (samples AN 19-24) forms a ridge dipping to the left in a drag fold. Note geologist for scale. See Fig. 4 for detailed log.

Fig. 9 - Details of the Himara Member, Al Mamalih section 2; a) desiccation cracks in red fine-grained sandstone; b) wave ripple crests with abundant surface trace fossils and bivalve casts preserved between the ripple crests. Scale is in centimetres.

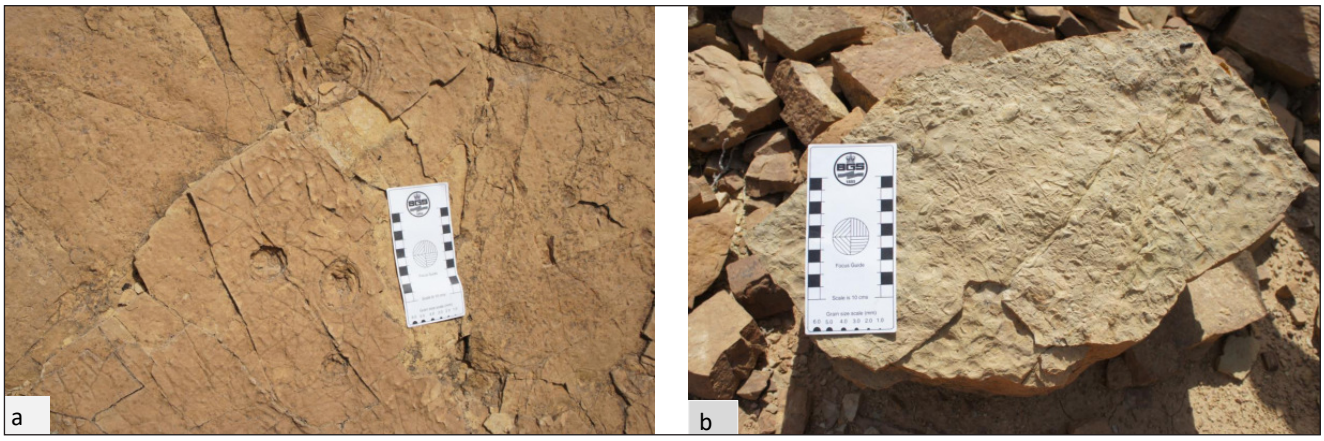

Fig. 10 - Details of the Nimra Member, Al Mamalih section 2; a) bedding plane surface (AN 21) of sandy limestone showing circular impressions (centre and middle right) interpreted as deflate algal domes (stromatolites); b) bedding plane surface showing abundant 'cuniform' linear trace fossils and casts of thin-shelled bivalves.

upward change to interbedded green fine-grained sandstone is accompanied by traces of thin-shelled bivalves, horizontal circular burrows and indeterminate linear surface-burrow traces. The boundary with the carbonate-rich Nimra Member is marked by green, green-grey and yellow-mauve, calcareous, fine-grained sandstone. Decalcified bivalves, conchostracans and burrow density increases upwards to the top of the ridge (Figs 4, 8) which is marked by a carbonate-rich bed (Samples AN 19 - AN 24). This bed is composed of partly dolomitized, fine-grained sandstone and packstone with fragments of echinoids, bivalves, crinoids; glauconite and phosphate peloids are common. Bedding planes reveal small domal stromatolites and abundant straight (or 'cuniform') surface burrows and casts of bivalves (Fig. 10). Foraminifera and conodonts are also present.

Section, 3 Dyke Plateau, Cliff/Track and Roadside Sections; Umm Irna and Ma'in formations.

As noted above, this revised section (Figs 5, 11a) is described in detail in Powell et al. (2016);

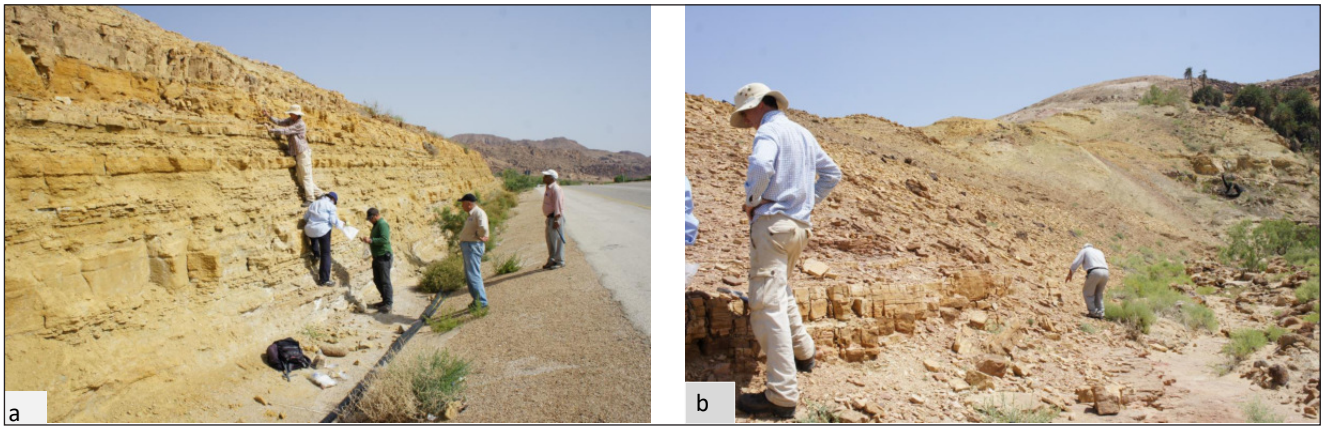

Fig. 11 - a) Roadside section showing the sandy limestone beds in the upper part (upper geologist is sampling bed AN 11. See Fig. 5 and Powell et al. (2016) for detailed log; b) Panorama Road section in the Upper Carbonate Member (Dardun Formation). Geologist in foreground is standing on beds AN 25 – 26. See Fig. 6 for detailed log.

however, during the present study the Roadside Section was extended downwards by 2 m, and the carbonate-rich beds in both sections were re-sampled for microfossils (AN 2 - AN 12). The latter comprise fine-grained, sandy limestone, partly dolomitized, and packstone/wakestone with fragments of gastropods, echinoderms, bivalves, serpulid worm tubes and phosphate granules. Sparse foraminifera are present in the Roadside Section.

Section 4, Panorama Road Section; Upper Carbonate Member, Dardun Formation

The Ma'in Formation is overlain by the mixed carbonate-siliciclastic Dardun Formation (Bandel & Khoury 1981). The latter comprises three members, in upward sequence: the Lower Carbonate Member (11 m thick), the Dardun Sandstone Member (15 m thick) and the Upper Limestone Member (23 m). In the study area, the lower two members form a steep cliff that is largely inaccessible. However, the upper member is accessible adjacent to the Panorama Road and was sampled for microfauna to constrain the age of the beds above the Ma'in Formation. The section (Figs 6, 11) comprises yellow, laminated beds of partly dolomitized packstone and wakestone with thin shelled bivalves, gastropods, crinoids, ooids, peloids and quartz grains with foraminifera in the upper 12.5 m (see below); these are interbedded with softer green, mauve and brown laminated calcareous sandy siltstone and fine-grained sandstone. Ripple cross-lamination and desiccation cracks are present in the lower 10 m. Bedding planes in the uppermost 4 m reveal abundant bivalves.

Biostratigraphy

Conodonts

Twenty-two samples (ca 3 to 4 kg) from the lower Nimra Member (Ma'in Formation) were investigated for conodonts (AN 2-24). Some of the samples (AN series) from the Dyke Plateau sections (Fig. 5) duplicate the samples reported in Powell et

AL MAMALIH GRABEN Section 1 **MA'IN Fm. NIMRA Mb.**	**AN13**	**AN14**	**AN15**	**AN16**	**AN17**
Hadrodontina aequabilis					
P_1	3	2	1	2	2
P_2	4	2	3	2	2
M	9	7	5	1	2
S_0	3	1			3
S_1	6	2	3		4
S_2	4	3	2		2
$S_{3/4}$	3	3	4		6
Fragments	7	7	8	3	9
Hadrodontina agordina					
P_1	2				1
P_2	2	1			1
M	10	1	1		7
S_0	3	2	1		1
S_1	1		3	1	4
S_2	1				3
$S_{3/4}$	3	1	2		9
Fragments	6		4	1	20
Indeterminated fragments	134	104	70	11	49

Tab. 1 - Numeric distribution of conodonts in Al Mamalih Graben Section 1.

AL MAMALIH GRABEN Section 2					
MA'IN Fm. NIMRA Mb.					
	AN19	**AN20**	**AN21**	**AN22**	**AN24**
Hadrodontina aequabilis					
P_1	1	2	2		
P_2		2	1		
M	11	9	6	3	
S_0	1				
S_1	4	4	4	3	
S_2	1	2	1	2	
$S_{3/4}$	3	2	4	2	
Fragments	12	26	26	6	
Hadrodontina agordina					
P_1	6	3	1	1	
P_2	2	1			
M	6	3	1		
S_0	1				
S_1	4	4		1	
S_2	3	2	1		
$S_{3/4}$	7	4	2	1	1
Fragments	21	13			
Hindeodus postparvus					
P_1	1				
$S_{3/4}$	3				
Indeterminate fragments	81	58	54	78	1

Tab. 2 - Numeric distribution of conodonts in Al Mamalih Graben Section 2.

DYKE PLATEAU_CLIFF/TRACK Section				
MA'IN Fm. NIMRA Mb.				
	AN4	**AN5**	**AN6**	**AN7**
		MS1	**MS2**	
Hadrodontina aequabilis				
P_1		2	2, 2	3
P_2		1	4	2
M	1	2, 1	8, 4	2
S_0				
S_1	1		4, 2	1
S_2	1fr.		2	1fr.
$S_{3/4}$		1	4	
Fragments	8	10, 2	18, 15	9
Hadrodontina agordina				
P_1				
P_2			1	1
M		2	2	2
S_0		1	1	
S_1			12	
S_2	1			1
$S_{3/4}$		2	3, 1	6
Fragments	5		10, 1	4
Indeterminated fragments		12	104, 12	74

Tab. 3 - Numeric distribution of conodonts in Dyke Plateau, Cliff/Track Section. AN and MS refer to sample series.

al. (2016) (see MS series shown in Fig. 5). In addition, the carbonates and sandy limestones from the stratigraphically higher Upper Carbonate Member of the Dardun Formation were also sampled.

The CAI (Colour Alteration Index, Epstein et al. 1977), produced by low-grade metamorphism of the organic matter in the conodonts is 1 to 1.5 corresponding to a burial temperature of 50°- 90°C. The conodont fauna is relatively abundant (Figs 12, 13) in the Mai'n Formation, but less abundant in the Dardun Formation (Tabs 1-5). Conodont identification took into account all the elements representing different locational notations in the conodont feeding apparatus. The abundant faunas have resulted in a refinement of the previous study (Powell et al. 2016). Elements in all stages of growth have been obtained in a good state of preservation. The abundance of fragments probably reflects winnowing and concentration of conodont apparatus in a shallow water environment. The conodont faunas in the Nimra Member (Ma'in Formation) are mostly from a 1 to 2 m interval of limestone and sandy limestone beds about 5 m above the base of the member. They consist predominantly of elements of the apparatus of *Hadrodontina aequabilis* Staesche, 1964 and *Hd. agordina* (Perri & Andraghetti, 1987); these species favoured shallow water environments and tolerated restricted marine conditions (Perri & Andraghetti 1987; Perri 1991; Farabegoli & Perri 1998; Nicora & Perri 1999; Perri & Farabegoli 2003; Perri et al. 2004; Farabegoli et al. 2007; Farabegoli & Perri 2012; Powell et al. 2016). Elements of all the locational notations of the septimembrate apparatus of the two species have been discriminated; some of them are described for the first time. One P_1 element of *Hindeodus postparvus* Kozur, 1990 has been identified in the Al Mamalih section 2 associated with a few fragments of a *Hindeodus* apparatus tentatively assigned to that species. We cannot exclude that in the examined material

DYKE PLATEAU_ROAD SIDE section MA'IN Fm. NIMRA Mb.	AN8 MS18	MS17	AN10
Hadrodontina aequabilis			
P_1			3
P_2	1		2
M	1, 3		9
S_0			
S_1			
S_2			
$S_{3/4}$	1		8
Fragments	2, 6	10	11
Hadrodontina agordina			
P_1			1
P_2			1
M			2
S_0			
S_1			4
S_2			2
$S_{3/4}$	1		2
Fragments	3		4
Indeterminated fragments	16, 5		58

Tab. 4 - Numeric distribution of conodonts in Dyke Plateau, Road Side Section. AN and MS refer to sample series.

PANORAMA ROAD Section DARDUM Fm. UPPER CARBONATE Mb.	AN28	AN29	AN30
Hadrodontina aequabilis			
P_1			
P_2			
M			
S_0			
S_1			
S_2			
$S_{3/4}$			
Fragments	4		1
Hadrodontina agordina			
P_1			
P_2			
M			
S_0	2		
S_1			
S_2			
$S_{3/4}$			
Fragments			
Indeterminated fragments		5	

Tab. 5 - Numeric distribution of conodonts in Panorama Road Section.

there may be elements belonging to other species. *Hadrodontina aequabilis* is a form-species described by Staesche (1964) from the Werfen Formation in the Dolomites (Southern Alps). Perri (1991), grouping conodont elements from the type area of that form-species, hypothesised a reconstruction of that apparatus. *Hadrodontina agordina,* also found in the Werfen Formation, was described as a multielement species by Perri & Andraghetti (1987). Both apparatuses were interpreted to consist of six elements. The Jordan material has allowed identification of all elements of the apparatus of the two species as being septimembrate. In the lowest sample of the Al Mamalih section 2 (AN 19) the two species co-occur with *Hindeodus postparvus* described by Kozur (1990) "from the Induan *isarcica* Zone, but with its main occurrence above this zone". Some forms previously included in *Isarcicella isarcica* Huckriede, 1958 (described from the Southern Alps) were excised and included in *Isarcicella staeschei* Dai & Zhang, 1989. The first occurrence of *Is. staeschei* is at stratigraphically lower levels. The former *isarcica* Zone was reconstituted as the *staeschei* and *isarcica* zones. These two marker taxa present morphologies that are easy to recognize and have short stratigraphical ranges. These species do not occur in sample AN 19. The *staeschei* and *isarcica* zones are the third and fourth biozones of the Early Triassic conodont biozonation proposed for the Southern Alps by Perri & Farabegoli (2003); they are easily correlatable with intervals in the Meishan D section, the GSSP of the Permian–Triassic boundary (Farabegoli et al. 2007; Farabegoli & Perri 2012). In the Southern Alps *Hadrodontina aequabilis* first occurs in the

Mazzin Member of the Werfen Formation in the *staeschei* Zone but with its main presence with, or immediately above, the highest occurrence of *Isarcicella isarcica*. *Hadrodontina agordina* enters in the Siusi Member of the Werfen Formation at stratigraphical levels about twenty-seven metres higher (Bulla section, Perri 1991; Farabegoli & Perri 1998; Perri unpubl.). We correlate the conodont-bearing beds of the Nimra Member (Jordan) with those in the Southern Alps above the *isarcica* Zone where *Hadrodontina aequabilis* and *Hd. agordina* co-occur within, and above, the stratigraphic range of *Hindeodus postparvus*. The genus *Hindeodus* became extinct during the Induan (Orchard 2007). Consequently, we date the conodont faunas from the lower Nimra Member as mid Induan.

Conodont systematic palaeontology

Genus *Hadrodontina* Staesche, 1964

Type species *Hadrodontina anceps* Staesche, 1964.

Hadrodontina aequabilis Staesche, 1964

Fig. 12, 1-19

P_1 element

1964 *Hadrodontina aequabilis* Staesche, p. 275, figs 11, 43-44.
1991 *Hadrodontina aequabilis* Staesche - Perri, Pa element, p. 36, pl. 2, figs 1a-c.
2004 *Hadrodontina aequabilis* Staesche - Perri et al., Pb element, figs 12a-b.
2012 *Hadrodontina aequabilis* Staesche - Farabegoli & Perri, Pa element, pl. 1, fig. 12.
2016 *Hadrodontina/Ellisonia* sp. - Powell et al., Pb element, fig. 9.9.

P_2 element

2016 *Hadrodontina aequabilis* Staesche - Powell et al., Pb element, figs 9.2 (gerontic form), 9.3.

M element

1991 *Hadrodontina aequabilis* Staesche - Perri, M element, p. 36, pl. 2, figs 3a-b, 4a-b, 5.
2004 *Hadrodontina aequabilis* Staesche - Perri et al., M element, fig. 16.
2012 *Hadrodontina aequabilis* Staesche - Farabegoli & Perri, M element, pl. 1, fig. 15.
2016 *Hadrodontina aequabilis* Staesche - Powell et al., M element, figs 9.1 (gerontic form), 9.10.

S_0 element no synonymy

S_1 element

1991 *Hadrodontina aequabilis* Staesche - Perri, Sb element, p. 36, pl. 2, figs 6a-b.
2004 *Hadrodontina aequabilis* Staesche - Perri et al., Sb element, figs 17a-c.
2012 *Hadrodontina aequabilis* Staesche - Farabegoli & Perri, Sb element, pl. 1, fig. 13.
2016 *Hadrodontina aequabilis* Staesche - Powell et al., Sb element, figs 9.5 and 9.6.

S_2 element

2016 *Hadrodontina aequabilis* Staesche - Powell et al., Pa element, figs 9.4a-c, figs 9.8a-c (gerontic forms).

$S_{3/4}$ element

1991 *Hadrodontina aequabilis* Staesche - Perri, Sc element, p. 36, pl. 2, figs 7a-c, 8a-b.
2004 *Hadrodontina aequabilis* Staesche - Perri et al., Sc element, figs 15a-b.
2012 *Hadrodontina aequabilis* Staesche - Farabegoli & Perri, Sc element, pl. 1, figs 14, 15
2016 *Hadrodontina aequabilis* Staesche - Powell et al., Sc element, figs 9.7, 9.11 (gerontic forms).

Diagnosis: Apparatus septimembrate comparable to the standard 15-element template of ozarkodinids by Purnell & Donoghue (1998) with element notations following Purnell et al. (2000) and Donaghue et al. (2008). It is composed by robust elements bearing discrete denticles with a mainly circular cross-section. They are characterized by a wide, flat to slightly concave basal cavity. A thin groove traverses the wide basal area and, in some elements, expands into a ring surrounding the pit.

Original description: Apparatus seximembrate with Pa element digyrate, Pb digyrate, M digyrate, Sa alate, Sb digyrate, Sc bipennate (Perri 1991). Big units with the characteristic anterior or outer face rounded. Peg-like denticles circular in cross-section. A secondary row of denticles smaller, and alternating with those of the main row, may be present. Abundant white matter. The elements of the apparatus are characterized by a wide, open and flaring basal cavity longitudinally crossed by growth strips and by a deep basal groove. Pit well visible.

Revised description. Septimembrate apparatus composed by P_1 angulate, P_2 breviform digyrate, M breviform digyrate, S_0 alate with posterior process, S_1 extensiform digyrate, S_2 breviform dygirate and $S_{3/4}$ bipennate elements.

Fig. 12 - Conodonts from the Nimra Member (Ma'in Formation) margins of the Dead Sea, Jordan.
Hadrodontina aequabilis Staesche, 1964.
1-4) P_1 elements, a. inner, b. outer views, 1 and 2 sample AN10, Road Side section; 3. sample AN17, 4. sample AN13, Al Mamalih section 1. 5-9) P_2 elements, 5. a., b. inner, c. outer, d. oral views respectively, 6 and 7. a. inner, b. outer views, sample AN17, 8. a. inner, b. outer views, sample AN15, Al Mamalih section 1; 9. a., b. inner, c. outer views, d. oral views respectively, sample AN20, Al Mamalih section 2. 10-12) M elements, a. inner, b. outer views, 10. sample 10, Road Side section; 11. sample AN13, 12. sample AN15, Al Mamalih section 1. 13) S_0 element, a. anterior, b. posterior views of one antero-lateral process, sample AN13, Al Mamalih section 1. 14-16) S_1 elements, 14. a. inner, b. outer, c. oral views respectively, 15. a. inner, b. outer, c. aboral views, sample AN13, 16. a. inner, b. outer views, sample AN15, Al Mamalih section 1. 17) S_2 element, a., b. inner, c. outer, d. aboral, e. oral views respectively, sample AN13, Al Mamalih section 1. 18-19) $S_{3/4}$ elements, a. inner, b. outer views, 18. sample AN10, Road Side section; 19. sample AN13, Al Mamalih section 1.
Scale bar 200 μm. All specimens at the same scale.

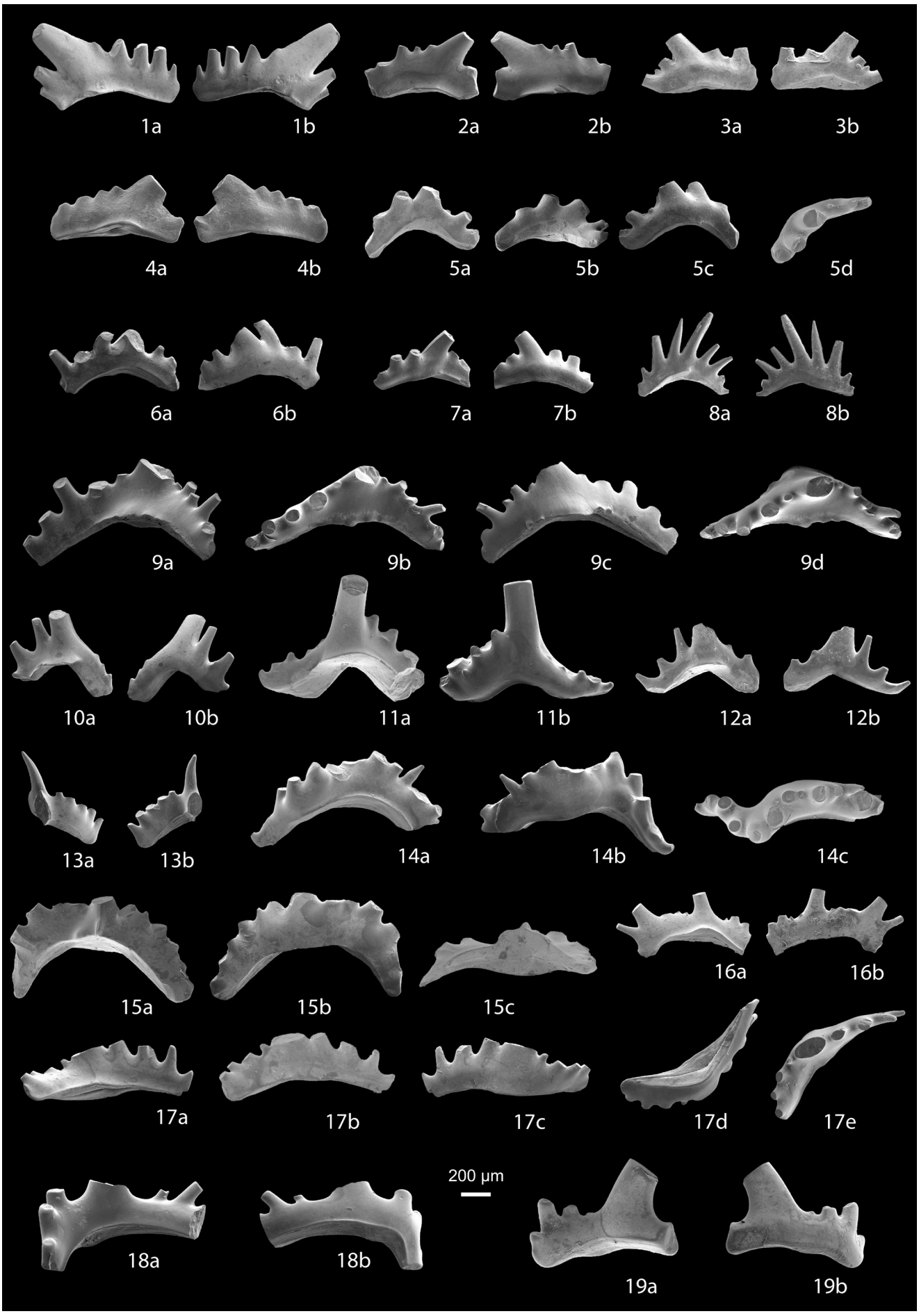
1a
1b
2a
2b
3a
3b
4a
4b
5a
5b
5c
5d
6a
6b
7a
7b
8a
8b
9a
9b
9c
9d
10a
10b
11a
11b
12a
12b
13a
13b
14a
14b
14c
15a
15b
15c
16a
16b
17a
17b
17c
17d
17e
200 µm
18a
18b
19a
19b

Elements can reach noteworthy dimensions. Denticles are discrete presenting a mainly circular section. A secondary row of smaller denticles, characteristic of the genus *Hadrodontina*, may be present, parallel to the main row. The basal area is at its widest at the pit for P_1, P_2, M and S_2, and near it for S_1 and $S_{3/4}$. Growth strips are well expressed. The morphology of the elements P_1 and P_2 is similar. P_1 is essentially straight, sometime slightly twisted. P_2 has longer processes and their distal extremities twist in opposite directions. A characteristic expansion like an ear (sometimes of striking size) is always present in M elements. It occurs at the base of the cusp where the two processes join.

P_1 element: angulate element straight to slightly twisted. The anterior process bears 4 to 5 denticles and is longer than the posterior one, bearing 2 to 3 denticles. The posterior process bends slightly downwards (Fig. 12, 1-4).

P_2 element: digyrate element with approximately equal processes. Distal extremities of the two processes twist in opposite directions (Fig. 12, 5-9).

M element: digyrate, arched element with slightly unequal processes. Characteristically has wide expansion at the base of the cusp (Fig. 12, 10-12).

S_0 element: alate with posterior process. Antero-lateral processes projected downwards, diverging at an angle of ca 90°. Each process bears 4 or 5 denticles (Fig. 12, 13).

S_1 element: extensiform digyrate with arched outline. Distal extremities of the two processes twist in opposite directions (Fig. 12, 14-16).

S_2 element: faintly arched, breviform digyrate with slightly unequal processes, bearing 3 or 4 denticles. The process anterior to the cusp is strongly bent inwards. Basal area wider below the cusp and sometimes considerably expanded (Fig. 12, 17).

$S_{3/4}$ element: bipennate with two disequal processes. The shorter anterior process is slightly curved inwards, sometime downwards, and bears 2-3 denticles. (Fig. 12, 18 and 19).

Remarks. On the basis of the description of the form-genus *Hadrodontina* by Staesche (1964), Sweet (1981) suggested a seximembrate apparatus "like that of genus *Furnishius*, but under sides of elements flattened rather than cuneiform and dimorphic Pa element". Reconstruction of the apparatus of *Hadrodontina* was figured by Sweet (in Robison 1981, fig. 101,1). He selected the form-species *Hadrodontina biserialis* Staesche, 1964 as Pa (= P_1) element of the *Hadrodontina* apparatus (Sweet in Robison 1981, fig. 101 - *Hadrodontina*-1e). Subsequently he located this element in Pb (= P_2) position (Sweet 1988, fig. 5.33). The form-species *Hadrodontina biserialis* is an angulate unit with a secondary row of denticles on outer side, parallel to main denticle series. Sweet (1988) asserted that the genus *Hadrodontina* as well as *Furnishius* and *Pachycladina* joined during the Early Triassic in shallow-water environments where they were associated with the genus *Ellisonia*, that had evolved during Pennsylvanian. The first three genera, illustrated by Sweet (1988, fig. 5.33), have a seximembrate apparatus with elements that are characterized by wide zones of recessive basal margin; the alate Sa elements lack a posterior process. Perri & Andraghetti (1987) and Perri (1991) reconstructed the apparatus of *Hadrodontina anceps* and *Hd. aequabilis,* respectively, from the Campil and Val Badia members and from the Mazzin and Siusi members of the Werfen Formation (Southern Alps). The material was collected from the type area where Staesche (1964) described the form-genus *Hadrodontina* and several form-species that formed the basis of the apparatuses in their reconstructions. According to Perri (1991) the elements of *Hadrodontina aequabilis* show a wide, open and flat basal area longitudinally crossed by a deep basal groove. Elements of the stratigraphically higher *Hd. anceps* display a wide recessive cuneiform basal area ending in a thin groove extending the entire length of the unit. The apparatus of *Hadrodontina* was described by Perri (1991) as seximembrate with robust elements bearing discrete peglike denticles containing white matter and a possible secondary row of denticles parallel to the main row. No element was known at that time for the S_2 location. Following Sweet (1988), Sa (=S_0) was supposed to lack a posterior process. No S_0 of *Hadrodontina anceps* and *Hd. aequabilis* was identified and figured from the Werfen Formation; in fact, the element identified as Sa and figured by Perri & Andraghetti (1987, Pl. 31 figs 4 a-b) in the apparatus of *Hadrodontina anceps* was assigned to P_1 by Donoghue et al. (2008, Appendix 2: Positional homology assignments). Koike et al. (2004) and Koike (2016) in their beautifully preserved and elegantly reconstructed apparatuses of *Hadrodontina* figured all S_0 as alate with a posterior process. In the Jordan conodont faunas, unfortunately incomplete elements (but clearly referable to S_0) showing traces of the posterior process are con-

sidered as belonging to the *Hadrodontina aequabilis* apparatus. Koike et al. (2004, p. 248, figs 8.1-8.8) on the basis of ellisonids elements collected from level 103 A of the Taho Formation, Shirokawa-cho, Higashiuwa-gun, Ehime Prefecture, southwestern Japan, just below the Smithian–Spathian boundary, reconstructed an apparatus consisting of eight elements named *Elissonia* sp. aff. *E. triassica*. Koike (2016, p. 164, figs 2.1-2.16) described and figured an apparatus also from the Taho Formation of Ehime Prefecture, but collected at Limestone Level 1612A and NK01 immediately below the Smithian–Spathian boundary. He referred this apparatus to *Hadrodontina aequabilis* including in the synonymy list all the elements of *Elissonia* sp. aff. *E. triassica* and some of the apparatus reconstructed by Perri (1991). According to Koike (2016) *Hadrodontina aequabilis* is composed of angulate (palmate) P_1 and P_2, digyrate M, triramous S_0, extensiform digyrate S_1 and S_2, and bipennate $S_{3/4}$, comparable to the standard 15-element template of ozarkodinids by Purnell & Donoghue (1998). Comparing *Hadrodontina aequabilis* figured by Koike (2016, fig. 2) with *Hadrodontina aequabilis* figured by Perri (1991, pl. 2, figs 1-8) and here in Fig. 12 the morphology of the elements of the two apparatuses is dissimilar. The apparatus of Perri (1991), assembled with elements from the Werfen Formtion of the Southern Alps, is morphologically close to the form-species *Hadrodontina aequabilis* by Staesche (1964, p. 275, figs 43–44). According to Staesche the form-species is characterized by: "underside slightly concave. The denticles are mostly quite evenly shaped and all inclined towards one end of the branch. The shape is somewhat twisted in itself "…"The branch is only weakly curved at the side, but slightly twisted. The lower surface is weakly concave and is longitudinally traversed by a flat keel. At the end of the posterior third of the length, it is expanded into a kind of ring in which the basal pit lies.". The last feature is visible in Staesche (1964, fig. 44) and in Perri (1991, Pl. 2, fig. 1c). The elements of Koike's apparatus - with the exception for that in Fig. 2.1 - seem to present reversed cuneiform basal areas closer to those of *Hadrodontina anceps* than to those of *Hd. aequabilis* of Perri (1991). The stratigraphical distributions also seem to be different. In the Southern Alps the species enters in the Induan *staeschei* Zone of Perri and Farabegoli (2003) and seems to extend no higher than the earliest Olenekian (Perri unpubl.). In northernmost Pakistan *Hadrodontina aequabilis* occurs in the *staeschei* and *isarcica* zones at Sakirmul and Torman Gol (Perri et al. 2004). In southwestern Japan it was found immediately below the Smithian–Spathian boundary. We do not follow the systematics proposed by Yang et al. (2014) where *Hadrodontina aequabilis* was synonymised with *Parafurnishius xuanhanensis*. In Pakistan (Perri et al., 2004), in the Southern Alps (Perri & Andraghetti 1987; Perri 1991; Farabegoli & Perri 1998; Nicora & Perri 1999; Perri & Farabegoli 2003; Farabegoli et al. 2007; Farabegoli & Perri 2012) and in Jordan (Powell et al. 2016; present paper) the P_1 element of *Parafurnishius xuanhanensis* has never been found, whereas elements of the apparatus of *Hadrodontina aequabilis* (Perri, 1991) are very abundant. On the basis of rich material from the Southern Alps, the reconstruction of the presumed apparatuses of the two species proposed in Perri & Andragetti (1987) for *Hadrodontina agordina* and in Perri (1991) for *Hadrodontina aequabilis*, our opinion concern two distinct multielement species. The abundant material found in Jordan successions permits revision of both species with identification of all elements of the hypothesised apparatuses.

In the Jordan material, huge gerontic forms with the basal area exaggeratedly expanded have been found (Powell et al. 2016, figs 9.1, 9.2, 9.4, 9.7, 9.8, 9.11). Similar forms occur also in the Siusi Mb. of the Werfen Fm. in the Southern Alps (Perri unpubl.).

Occurrence. Ma'in Formation, Nimra Member: Al Mamalih Graben section 1, samples AN 13–AN 17; Al Mamalih section 2, samples AN 19–AN 22; Cliff/Track section, samples AN 4, AN 5 + MS 1, AN 6–AN 7 + MS 2; Separate Cliff section to the north, sample AN 1; Road Side section, samples AN 8 + MS 18, MS 17, AN 10. Dardun Formation, Upper Carbonate Member: Panorama Road section, samples AN 28, AN 30.

Age. Early Triassic, Induan to ?earliest Olenekian.

Hadrodontina agordina
(Perri & Andraghetti, 1987)

Fig. 13, 1-27

P_1 element no synonymy.

P_2 element

1991 *Ellisonia agordina* Perri & Andraghetti - Perri, Pb element, p. 34, pl. 1, figs 2a-b.

M element
1987 *Ellisonia agordina* Perri & Andraghetti, M element, p. 304, pl. 30, figs 3a-b.
1991 *Ellisonia agordina* Perri & Andraghetti - Perri, M element, p. 34, pl. 1, figs 3a-b.
S_0 element
1987 *Ellisonia agordina* Perri & Andraghetti, 1987, Sa element, p. 304, pl. 30, figs 4, 5.
1991 *Ellisonia agordina* Perri & Andraghetti - Perri, Sa element, p. 34, pl. 1, fig. 4.
S_1 element
1987 *Ellisonia agordina* Perri & Andraghetti, Sb element, p. 304, pl. 30, figs 6a-b.
1991 *Ellisonia agordina* Perri & Andraghetti - Perri, Sb element, p. 34, pl. 1, figs 5a-b.
S_2 element
1987 *Ellisonia agordina* Perri & Andraghetti, Pa element, p. 304, pl. 30, figs 1a-b.
1987 *Ellisonia agordina* Perri & Andraghetti, Pb element, p. 304, pl. 30, figs 2a-b.
1991 *Ellisonia agordina* Perri & Andraghetti - Perri, Pa element, p. 34, pl. 1, figs 1a-b.
$S_{3/4}$ element
1987 *Ellisonia agordina* Perri & Andraghetti, Sc element, p. 304, pl. 30, figs 7a-b.

Original diagnosis: Species with a seximembrate apparatus characterized by an inflated rib at mid-height of the elements.

Revised diagnosis: Apparatus septimembrate comparable to the standard 15-element template of ozarkodinids by Purnell & Donoghue (1998) with element notations following Purnell et al. (2000) and Donaghue et al. (2008). Elements are short and mainly squat with discrete robust denticles. Elements have an inflated rib at about mid-height of the anterior side in the S_0 element, and of the outer side in other elements. The wide reversed basal area is flat to slightly protruding and traversed by a thin basal groove crossing a small pit; growth strips are easily discriminated.

Original description: Seximembrate apparatus constituted by a carminte Pa element, Pb digyrate and bowed out, M digyrate, Sa alate with posterior process, Sb digyrate, Sc bipennate with long posterior process and shorter laterally deflected anterior process (Perri & Andraghetti 1987).

Revised description. Septimembrate apparatus composed by P_1 angulate, P_2 breviform digyrate, M breviform digyrate, S_0 alate with posterior process, S_1 extensiform digyrate, S_2 breviform dygirate and $S_{3/4}$ bipennate elements.

P_1 element: angulate mainly squat and straight with maximum width at mid-unit, tapering along the posterior process. The anterior process bears 4 or 5 denticles increasing in size towards the cusp, the posterior bears 2 or 3 denticles. The posterior process bends slightly downwards. Basal area wide and flat, sometimes faintly arched. Swelling along the unit is characteristic (Fig. 13, 1-7).

P_2 element: breviform digyrate, presenting the anterior process twisted inwards and bearing 3–4 denticles. It is longer than the posterior process behind the cusp twisted outwards and bearing 2 to 3 denticles. Cusp well developed, clearly differentiated. Characteristic swelling along the entire unit (Fig. 13, 8 and 10).

M element: breviform digyrate with processes of nearly equal length forming an angle wider than 90°. Cusp well developed and differentiated (Fig. 13, 9 and 11-13).

S_0 element: alate with arched denticulate posterior process. The short antero-lateral processes form an angle of 180° and display the characteristic swelling of the species on the anterior side. Cusp well developed and differentiated (Fig. 13, 14-16).

S_1 element: extensiform digyrate with two processes of different length. Distal extremities of the two processes twist in opposite direction. Basal area reversed and arched. Swelling typical of the species on the outer side in correspondence with the cusp (Figs 13, 17).

S_2 element: breviform dygirate, short, bended and slightly twisted with flat basal area. Short-

Fig. 13 - Conodonts (continued) from the Nimra Member (Ma'in Formation) along the margins of the Dead Sea, Jordan.
Hadrodontina agordina (Perri & Farabegoli, 1987)
1-7) P_1 elements, 1. a. inner-aboral, b. outer, c. aboral, d. oral views respectively, 2. a. inner, b. aboral, c. oral views, sample AN10, Road Side section; 3. a. inner, b. outer views, 4. a. inner, b. outer, c. oral views, sample AN13, 5. a. inner, b. outer, c aboral views, sample AN15, Al Mamalih section 1, 6. a. inner-oral, b. outer, c. inner-aboral views, 7. a. inner, b. outer views, sample AN20, Al Mamalih section 2. 8, 10) P_2 elements, 8. a. inner, b. outer views, sample AN17, 10. a. inner, b. outer, c. aboral views, sample AN13, Al Mamalih section 1. 11-13) M elements, 11. a. inner, b. inner-aboral, c. outer views, sample AN17, 13. a. inner, b. outer views, sample AN13, Al Mamalih section 1; 12. a. inner-aboral, b. outer views, sample AN19, Al Mamalih section 2. 14-16) S_0 elements, 14. a. oral, b. lateral views, sample AN15, 16. a. oral, b. anterior views, sample AN17, Al Mamalih section 1; 15. lateral view, sample AN19, Al Mamalih section 2. 17) S_1 element, a. inner, b. outer, c. oral views, sample AN17, Al Mamalih section 1. 18-21) S_2 elements, 18. a. inner, b. outer, c. aboral views, 19. and 20. a. inner, b. outer, c. oral views, sample AN19, Al Mamalih section 2; 21. a. inner, b. oral views, sample AN17, Al Mamalih section 1. 22-27) $S_{3/4}$ elements, 22. a. inner, b. outer views, sample 19, Al Mamalih section 2; 23. a. inner, b. outer, c. aboral views, 24. a. inner, b. outer, c. oral views, sample AN17, Al Mamalih section 1; 25. a. inner, b. outer, c. aboral views, sample AN19, 26. a. inner, b. outer, c. aboral views, 27. a. inner, b. outer views, sample AN20, Al Mamalih section 2.
Hindeodus postparvus Kozur, 1990
28) a. oral, b. aboral, c. lateral views, sample AN19, Al Mamalih section 2.
Scale bar 200 μm. All specimens at the same scale.

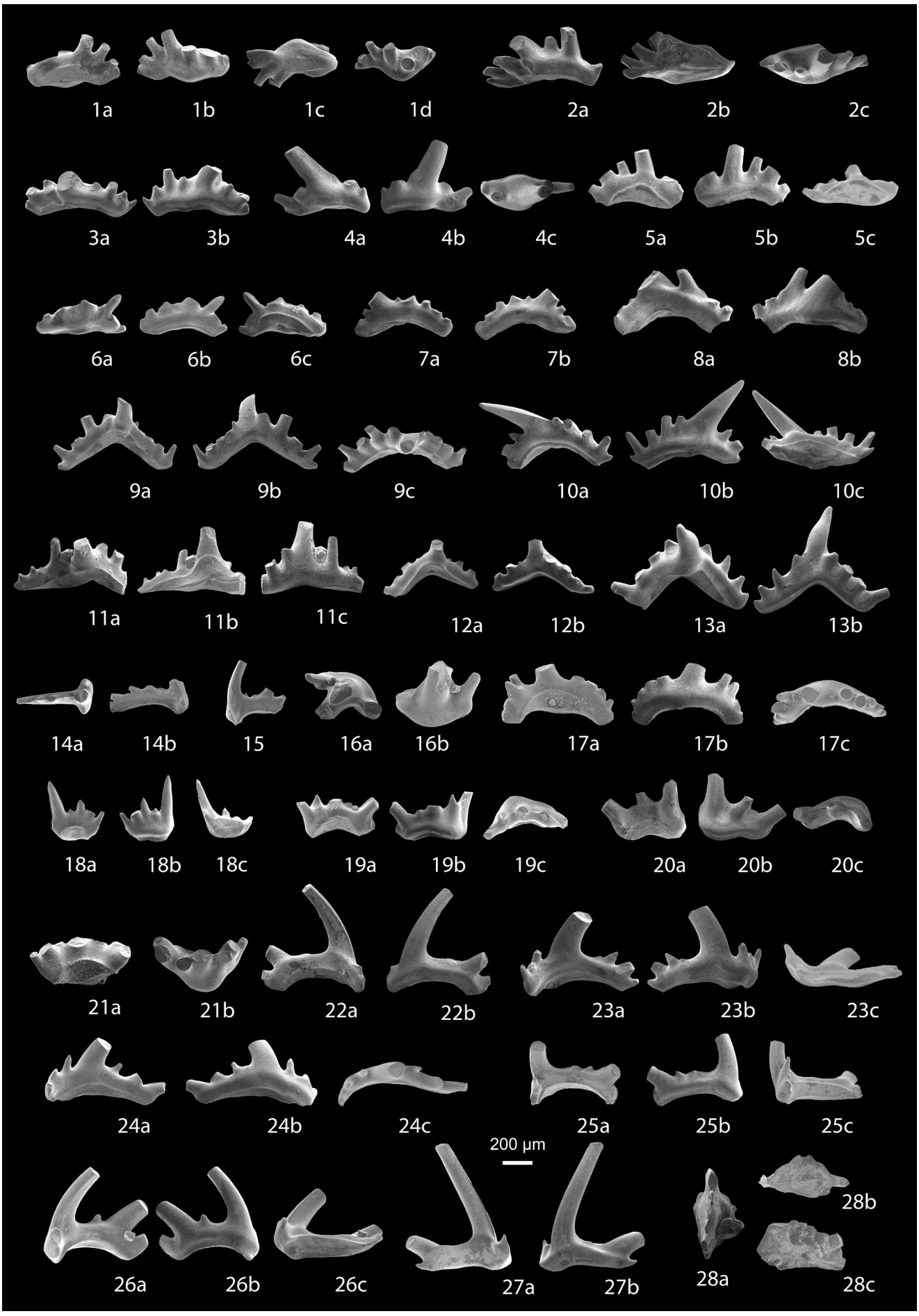
1a
1b
1c
1d
2a
2b
2c
3a
3b
4a
4b
4c
5a
5b
5c
6a
6b
6c
7a
7b
8a
8b
9a
9b
9c
10a
10b
10c
11a
11b
11c
12a
12b
13a
13b
14a
14b
15
16a
16b
17a
17b
17c
18a
18b
18c
19a
19b
19c
20a
20b
20c
21a
21b
22a
22b
23a
23b
23c
24a
24b
24c
25a
25b
25c
200 µm
26a
26b
26c
27a
27b
28a
28b
28c

er process bends inwards at the point of juncture with the cusp. Swelling on the outer side characteristic, corresponding with the cusp, similar to that of the other S elements (Figs 13, 18-21).

$S_{3/4}$ element: bipennate with the shorter anterior process bent inwards and bearing a few denticles. Posterior process with flat basal area. Swelling on the outer side characteristic, corresponding with the cusp (Figs 13, 22-27).

Remarks. Perri & Andraghetti (1987, p. 303, pl. 30) described the new species *E. agordina* from the Lower Triassic succession of the Southern Alps and hypothesised a seximembrate apparatus. The new species was found in the Siusi Member of the Werfen Formation. The presence of a posterior process in the Sa alate element induced Perri & Andraghetti to refer the new species to genus *Ellisonia*. According to Sweet (1988, p. 85) the alate Sa (=S_0) elements of *Hadrodontina* lack a posterior process - the converse in those of *Ellisonia*. Presence or absence of the posterior process in the S_0 element is not diagnostic (Donoghue et al. 2008). According to Koike (2016, p. 167) "S_1 element with slightly arched processes without bending in the outer lateral process is an important clue in distinguishing the genus *Ellisonia* from other genera of Triassic ellisonids". Study of Lower Triassic material from Jordan has allowed the identification of seven morphologically distinct types of elements suggesting that the apparatus is septimembrate comparable to the standard 15-element template of ozarkodinids of Purnell & Donoghue (1998). The morphology of the elements constituting the apparatus induces us to assign the species to the genus *Hadrodontina* as also did Koike (2016, fig. 1) though questionably. The P_1 element of *Hadrodontina agordina* is here described and figured for the first time. A P_1 element was not found in the Southern Alps associations. Elements previously assigned to P_1 (=Pa, Perri & Andraghetti 1987, pl. 30, figs 1a-b; Perri 1991, pl. 1, figs 1a-b) are now identified as juvenile S_2 elements.

Occurrence. Ma'in Formation, Nimra Member: Al Mamalih Graben section 1, samples AN 13–AN 17; Al Mamalih section 2, samples AN 19–AN 22, AN 23; Cliff/Track section, samples AN 4, AN 5 + MS 1, AN 6–AN 7 + MS 2; Separate Cliff section to the north, sample AN 1; Road Side section, samples AN 8 + MS 18, AN 10. Dardun Formation, Upper Carbonate Member: Panorama Road section, sample AN 28.

Age. Early Triassic, Induan to ?earliest Olenekian.

Genus *Hindeodus* Rexroad & Furnish, 1964

Type species *Trichonodella imperfecta* Rexroad, 1957

(= *Spathognathodus cristulus* Youngquist & Miller, 1949).

Hindeodus postparvus Kozur, 1990

Fig. 13, 28

1990 *Hindeodus postparvus* Kozur, p. 400, holotype figured by Kozur, 1977, pl. 1, fig. 20.
1996 *Hindeodus postparvus* Kozur - Kozur, p. 98, pl. 2, figs 9–10 *cum synonymy*
1998 *Hindeodus postparvus* Kozur - Orchard and Krystyn, pl. 6, fig. 1
2009 *Hindeodus postparvus* Kozur - Chen et al., fig. 11: 6–12
2011 *Hindeodus postparvus* Kozur - Kolar et al., pl. 7, fig. 1
2014 *Hindeodus postparvus* Kozur - Jiang et al., pl. 1: 2–3
2015 *Hindeodus postparvus* Kozur - Brosse et al. fig. 3: H–N

Diagnosis: Pa element small and arched with, commonly, a large cusp and six to seven, rarely large, highly fused denticles with strongly diverging inclination resulting in a distinctly arched upper profile of the Pa element. Large cup is present. M element, the only other easily identifiable part of the apparatus, shows a characteristic denticulate posterior process (Kozur 1996).

Remarks. The only P_1 element found is poorly preserved. We nevertheless assigned it to *Hindeodus postparvus* because its lower margin is arched in accordance with the widest point of the basal cavity and because of the robust, radially-arranged denticles. The species is rather rare. Kozur (1996) reported the species in Malaysia (in Metcalfe's 1995 material) and in Transcaucasia it first appears in the *isarcica* Zone, but its principal occurrence is above this zone. He proposed a *postparvus* Zone immediately above the *isarcica* Zone; it correlates with the lower part of the *aequabilis* Zone of Perri & Farabegoli (2003) in the Southern Alps. The *isarcica* Zone of Kozur (1996) is equivalent to the *staeschei* plus *isarcica* zones of Perri & Farabegoli (2003). Chen et al. (2009) reported *Hindeodus postparvus* in association with *Isarcicella staeschei* from the Daye Formation in the Dawen section, Great Bank of Guizhou, Guizhou Province, South China. Therefore, the first appearance datum (FAD) of the species is in the *staeschei* Zone. According to Kolar-Jurkovsek et al. (2011) in the Lukac section in western Slovenia, *Hindeodus postparvus* enters in the *staeschei–isarcica* Zone. The extinction of *Isarcicella isarcica* defines the base of the *postparvus* Zone, but its principal occurrence is above this zone. They define the upper limit of the biozone coincident with the last occurrence datum of *Hindeodus postpar-*

vus. Brosse et al. (2015) report the species from the Griesbachian Luolou Formation in the Wuzhuan section (Nanpanjiang Basin, Guangxi, South China) from a level stratigraphically higher than *Isarcicella isarcica* in association with representatives of *Hindeodus parvus*. Lyu et al. (2017) define a *Hindeodus postparvus* Zone characterized by the co-occurrence of *Hindeodus postparvus*, *Hi. parvus*, and locally *Clarkina planata* in the upper Griesbachian of the western Hubei Province, South China. The range of the genus *Hindeodus* is Early Carboniferous (Tournaisian) to Early Triassic (Induan) (Orchard 2007). *Hindeodus postparvus* may be the last representative of the genus.

A few fragments found in association with the P_1 element showing characteristics of the ramiforms of *Hindeodus* have been tentatively identified as $S_{3/4}$ of the *Hindeodus postparvus* apparatus.

Occurrence. Ma'In Formation, Nimra Member: Al Mamalih section 2, sample AN 19.

Age. Induan.

Foraminifera

Thin section analysis of thirty-five samples from the studied stratigraphical sections provides important biostratigraphical data from the foraminifera that allows us to define the age of the Nimra Member (Ma'in Formation) and the stratigraphically higher Upper Carbonate Member (Dardun Formation). The foraminiferal analysis was not performed on samples of the Cliff/Track section (Nimra Member) (Fig. 5) because the samples were not productive. In the other three analysed sections, the diversity of benthic foraminiferal assemblages is low, although they seem to be characteristic, and similar to those from other sections of the Tethyan domain (Song et al. 2016 with bibliography).

Foraminifers are present in the Dyke Plateau Roadside section (Powell et al. 2016) in samples AN 8 and 11 (Figs 5, 11a); they are sparse and are represented respectively by the taxa *Postcladella* gr. *kalhori* (Brönnimann et al. 1972) and *Earlandia* spp. This assemblage has been recognised in many regions around the world mostly within the microbialite microfacies that follows the Permian-Triassic extinction event (Altıner et al. 1980; Altıner & Zaninetti 1981; Groves et al. 2005; Groves et al. 2007; Song et al. 2009). On the basis of these co-occurrences, the studied interval of the Nimra Member (from sample AN 8 to AN 11; Dyke Plateau/Roadside sections) is referred to the Induan.

In the broadly coeval Nimra Member of the Al Mamalih sections (Figs 3-4, 7-8), we only record the presence of the new species *Ammodiscus jordanensis* n. sp. (Fig. 14) in samples AN 14 (Section 1) and AN 20 (Section 2). Their age has been indirectly referred to the Induan, because these samples are correlated with the similar carbonate beds of Nimra Member (Dyke Plateau Roadside section) which is considered Induan in age on the basis of the *P.* gr. *kalhori-Earlandia* spp. assemblage.

The Panorama Road section (Figs 6, 11b) through the Upper Carbonate Member of the Dardun Formation records important bioevents. The first occurrence (FO), in sample AN 29, of *Postcladella* gr. *kalhori* (Fig. 15), associated with *Ammodiscus jordanensis* n. sp., *Ammodiscus* spp., and *Glomospirella* sp. indicates an Induan age. In the majority of lowest Triassic deposits of the Tethyan domain, after the P/T boundary, foraminifers are completely absent. The first record of foraminifers is represented by opportunistic, abundant, morphologically simple and long-ranging forms, such as *Earlandia* spp. and *Postcladella* gr. *kalhori* (Fig. 15). This assemblage can be identified as composed by 'disaster forms' (sensu Fischer & Arthur 1977) in which, based on similar characteristics, *Ammodiscus jordanensis* n. sp. can also be included. Sample AN 31, about 8 m above, records the FO of *Citaella pusilla* (Ho, 1959; Ueno et al. 2018) (Fig. 15) which is also present in AN 32. Taking into account that the assemblage *Postcladella* gr. *kalhori-Earlandia* spp.-*Ammodiscus jordanensis* n. sp. is considered as Induan in age, whilst *Citaella pusilla* is typical of the Olenekian (Broglio Loriga et al. 1990; Rettori 1995), the stratigraphic interval, from sample AN 29 to AN 32 of the Upper Carbonate Member, spans the Induan-Olenekian boundary interval.

Foraminifera Systematic Palaeontology (V. Gennari and R. Rettori)

Sample AN 14 collected from 6.5 m above the base of the Nimra Member yielded a new foraminifera species, *Ammodiscus jordanensis* n. sp., described below.

Phylum **FORAMINIFERA** d'Orbigny, 1826
Class **Spirillinata** Mikhalevich, 1992
(=Tubothalamea Pawlowski et al., 2012, part, in Adl et al., 2012)

Subclass **Ammodiscana** Mikhalevich, 1980
Order **Ammodiscida** Mikhalevich, 1980
Superfamily Ammodiscoidea Reuss, 1862
Family Ammodiscidae Reuss, 1862
Type genus: *Ammodiscus* Reuss, 1862
Type species: *Ammodiscus infimus* Bornemann, 1874

Ammodiscus jordanensis n. sp.

Fig. 14, 1-7

1959 *Ammodiscus multivolutus* Reitlinger - Ho, p. 419, pl. 1, fig. 22-24
? 1959 *Ammodiscus multivolutus* Reitlinger - Ho, p. 420, pl. 2, fig. 1-2
1975 *Ammodiscus* sp. - Gazdzicki et al., pl. 1, fig. 1
1983 *Ammodiscus multivolutus* Reitlinger - Salaj et al., pl. 1, fig. 1, pl. 6, fig. 1-2
1987 *Ammodiscus* cf. *inaequabilis* Styk - Oravecz-Scheffer, p. 165, pl. 15, fig. 2
1988 *Ammodiscus multivolutus* Reitlinger - He, p. 94, pl. 2, fig. 3-4
1997 *Ammodiscus multivolutus* Reitlinger - Bucur et al., p. 46, pl. 3, fig. 15

Derivation of the name: The new species is named from Jordan.

Holotype: The specimen in axial section figured in Fig. 14, 1, from sample AN 14 (Al Mamalih Section 1). The type material is deposited at the Dipartimento di Fisica e Geologia, University of Perugia (Italy).

Material: Specimens from sample AN 20 (Al Mamalih section 2) and from sample AN 29 (Panorama Road section).

Type level: Lower Triassic (Induan), about 6.5 m above the base of the Nimra Member (Ma'in Formation) in the Al Mamalih Section 1 (Fig. 3).

Type locality: Al Mamalih area, ca 5 km north of Wadi Mujib delta, Jordan.

Assemblage: In the type material the new species *Ammodiscus jordanensis* n. sp. has been recorded associated with *Postcladella* gr. *kalhori* (Brönnimann et al. 1972), *Glomospirella* sp., *Ammodiscus* spp., thin shelled bivalves, echinoderm fragments and conchostracans.

Diagnosis: Species of the genus *Ammodiscus* characterised by six to seven whorls sometimes oscillating. Asymmetrical umbilical depressions. Tubular chamber rectangular to circular in the last whorl.

Description. Test free, discoidal, composed by 6 to 7 evolute whorls. Globular proloculus followed by a second, undivided, tubular chamber, planispirally coiled, sometimes oscillating. Depressed umbilici and one umbilicus is more depressed than the other. The tubular chamber, rectangular in outline, slowly increases in width but not in height; in the adult forms, in the last whorl, the tubular chamber becomes nearly circular in outline. Aperture simple at the end of the tubular chamber. The wall is thin, grey, finely agglutinated.

Dimensions (μm)

Diameter of the test: 250-480.
Width of the test in the juvenile stage: 16-39.
Width of the test in the adult stage: 40-60.
Thickness of the wall: 4.5.

Remarks. The new species differs from *Ammodiscus multivolutus* Reitlinger, 1949 from the Carboniferous of Russia because the latter is characterised by the height of the tubular chamber, which gradually increases during the growth and by the presence of one flat side. Furthermore, regarding the nature of the wall, the species *multivolutus* seems not to belong to the genus *Ammodiscus* Reuss as stated by Krainer et al. (2005) who referred the species to the genus *Cornuspira* Schultze, subgenus *Turrispiroides* Reitlinger, (Miliolida). *Ammodiscus jordanensis* n. sp. can be distinguished from the Lower Triassic *Ammodiscus parapriscus* Ho, 1959 because the Chinese species has a small test size, the tubular chambers increase rapidly, and the number of whorls is reduced. Ho (1959) also figured *Ammodiscus multivolutus* that we consider to be synonym of *Ammodiscus jordanensis* n. sp. under the name *Ammodiscus multivolutus.* Several other authors reported specimens recorded in the Triassic of Tethyan domain that we have, herein, included in the new species *Ammodiscus jordanensis* n. sp. The peculiar silhouette of the new species allows the taxon to be easily recognised. It could be erroneously confused with un-centred cross-sections of Triassic species of the genus *Glomospirella* Plummer, characterised by a very reduced initial glomospiroid stage, such as specimens referred by Ho (1959) to *G. spirillinoides* (Grozdilova & Glebovskaia, 1948) or *G. vulgaris* Ho, 1959. The absence of any glomospiroid initial stage in all the studied specimens and the finely agglutinated nature of the wall justify the attribution of the species *jordanensis* to the genus *Ammodiscus*.

Fig. 14 - Foraminifera from the Induan Nimra Member (Mai'in Formation) (AN 8, 11, 14, 20) and Upper Carbonate Member (Dardun Formation) (AN 29); scale bar 50 μm
1) *Ammodiscus jordanensis* n. sp., Holotype AN 14;
2) *Ammodiscus jordanensis* n. sp. AN 20;
3) *Ammodiscus jordanensis* n. sp. AN 29;
4) *Ammodiscus jordanensis* n. sp. AN 29;
5) *Ammodiscus jordanensis* n. sp. AN 29;
6) *Ammodiscus jordanensis* n. sp. AN 29;
7) *Ammodiscus jordanensis* n. sp. AN 29;
8) *Glomospirella* sp. AN 29;
9) *Postcladella* gr. *kalhori* (Brönnimann et al. 1972) AN 29;
10) *Postcladella* gr. *kalhori* (Brönnimann et al. 1972) AN 29;
11) *Postcladella* gr. *kalhori* (Brönnimann et al. 1972) AN 8;
12) *Earlandia* spp. AN 11.

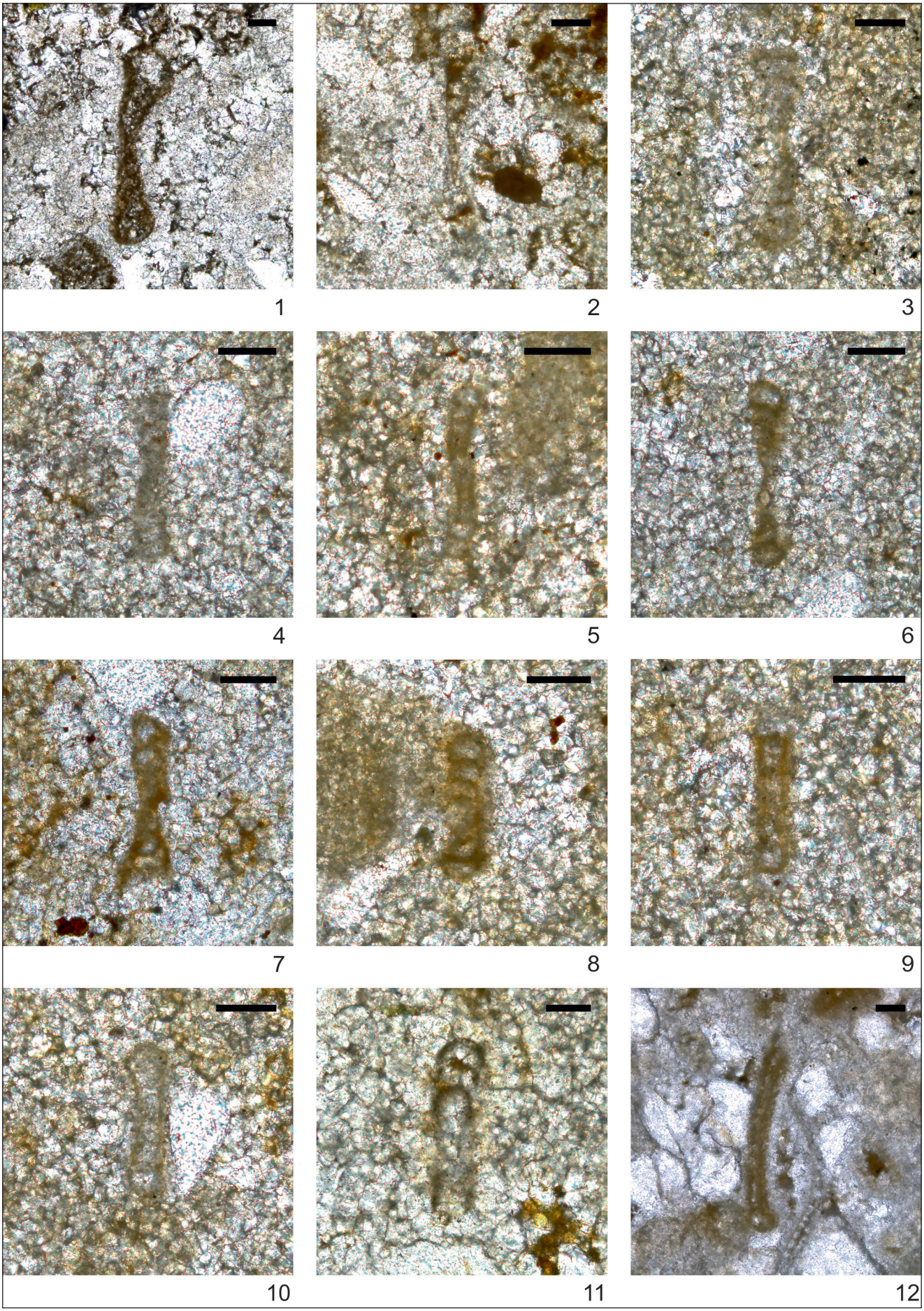
1
2
3
4
5
6
7
8
9
10
11
12

Stratigraphic and geographic distribution. Induan of Jordan; Lower Triassic of South Szechuan, Jiangsu and Anhui Provinces ("Chialingchiang Limestone" s.l.), China; Middle Triassic of western and southern Carpathians and of Transdanubian Central Range (Poland, Romania and Hungary).

Bivalves

The studied material was collected from bed NA 51 of the Al Mamalih section 2 (Nimra Member of the Ma'in Formation) (Fig. 16). The bivalves are mostly preserved as internal moulds and outer casts. All the specimens are disarticulated, but fragmentation is very low, suggesting their burial was rapid. The bivalve assemblage has a low diversity. It contains the following three genera: *Claraia, Unionites* and *Eumorphotis*. The latter genus is represented by only a left valve. *Unionites* is present as monotypic assemblages or is associated with the other two genera. Some *Claraia* valves are encrusted by tubeworms which can be referred to microconchids, a disaster taxon occurring both in shallow and deep marine environments (e.g., He et al. 2012).

The occurrence of a *Claraia* species (*Claraia bittneri* Ichikawa, 1958) of the *C. aurita* group allows the correlation of the Nirmra Member Claraia beds with the *Claraia aurita* group subzone of the Dolomites (Broglio Loriga et al. 1983). This biostratigraphic unit characterizes the middle Siusi Member of the Werfen Formation. Its upper boundary corresponds to the disappearance of *Claraia* and other "dead clade walking" (Jablonski 2002; e.g. the bellerophontid *Warthia* Kaim & Nützel 2011). This Dinerian biotic crisis is associated by depleted $\delta^{13}C$ values (Foster et al. 2017). In the Bulla section, the disappearance of *Claraia* occurs at about 70 m above the base of Siusi Member (samples BU 49 – BU 50 of Farabegoli & Perri 1998; Posenato 2008a).

In this paper the adopted Bivalvia classification follows He et al. (2007), Carter et al. (2011, simplified) and Hautmann et al. (2013).

Bivalve Systematic palaeontology

Class **Bivalvia** Linnaeus 1758 in 1758-1759
Order **Pectinida** J. Gray, 1854a
Superfamily Pterinopectinoidea Newell, 1938
Family Pterinopectinidae Newell, 1938
Genus *Claraia* Bittner, 1901
Type species: *Posidonomya clarae* Emmrich, 1844

Claraia bittneri Ichikawa, 1958

Fig. 16, 1-6, Tab. 6

1901 *Pseudomonotis (Claraia) tridentina* Bittner, p. 589-591, pl. 24, figs 1-9.
1927 *Pseudomonotis (Claraia) tridentina* Bittner - Ogilvie Gordon, pl. 1, fig. 5a-e.
1935 *Claraia tridentina* Bittner - Leonardi, p. 62, pl. 3, fig. 10 (not fig. 9 = *C. aurita*).
1958 *Claraia bittneri* Ichikawa, p. 138.
1960 *Claraia tridentina* Bittner - Leonardi, pl. 8, fig. 6.

Material: A dozen valves represented by outer casts and internal moulds are available. Only few specimens are entire and not apparently deformed (five right and four left). The majority of valves are located on the lower surface of a fine-grained, cross-bedded sandstone bed (A 1- A 12). They are associated with rare *Eumorphotis* and *Unionites* specimens. A right valve (E1), located on the upper surface of a small slab from a sandstone bed, is slightly deformed.

Measurements (in mm) are presented in Tab. 6.

Specimen	Length	Height	Thickness	LA	Tv	L/H	T/H
A1	45.9	43.1	8.5	18.5	LV	1.06	0.20
A5	42.9*	36.3*	3.5*	13.7*	RV	-	-
A7	37.4	35.5	6.6	12.7	LV	1.05	0.19
A8	41.4	35.1	4.3	13.9	RV	1.18	0.12
A9	37.0*	37.3	5.5	10.6*	RV	-	0.15
A10	34.0*	32.2*	4.5	12.4*	RV?	-	-
A11	36.4*	29.8*	3.2*	11.8*	LV	-	-
A12	29.5	-	4,6	11.8	RV	-	-
B1	39.8*	41.2	8	14.5	LV	0.97	0.19
E1	35.8	30.2	5.5*	11.5	RV	1.19	-

Tab. 6 - Shell measurements for *Claraia bittneri* Ichikawa, 1958.
Abbreviations: LA, distance of the umbo from the anterior margin; * incomplete specimen; LR, right valve; LV, left valve; Tv, type of valve.

Fig. 15 - Foraminifera from the Induan-Olenekian Upper Carbonate Member (Dardun Formation) (AN 29, 30,31, 32); scale bar 50 μm
1) ? *Postcladella* gr. *kalhori* (Brönnimann et al. 1972) AN 29;
2) *Ammodiscus* spp. AN 29;
3) *Ammodiscus* spp. AN 29;
4) *Postcladella* gr. *kalhori* (Brönnimann et al. 1972) AN 29;
5) *Ammodiscus* spp. AN 29;
6) *Postcladella* gr. *kalhori* (Brönnimann et al. 1972) AN 29;
7) ? *Glomospirella* sp. AN 30;
8) *Citaella pusilla* (Ho, 1959) AN 31;
9) *Citaella pusilla* (Ho, 1959) AN 31;
10) *Citaella pusilla* (Ho, 1959) AN 31;
11) *Citaella pusilla* (Ho, 1959) AN 32;
12) *Citaella pusilla* (Ho, 1959) AN 32.

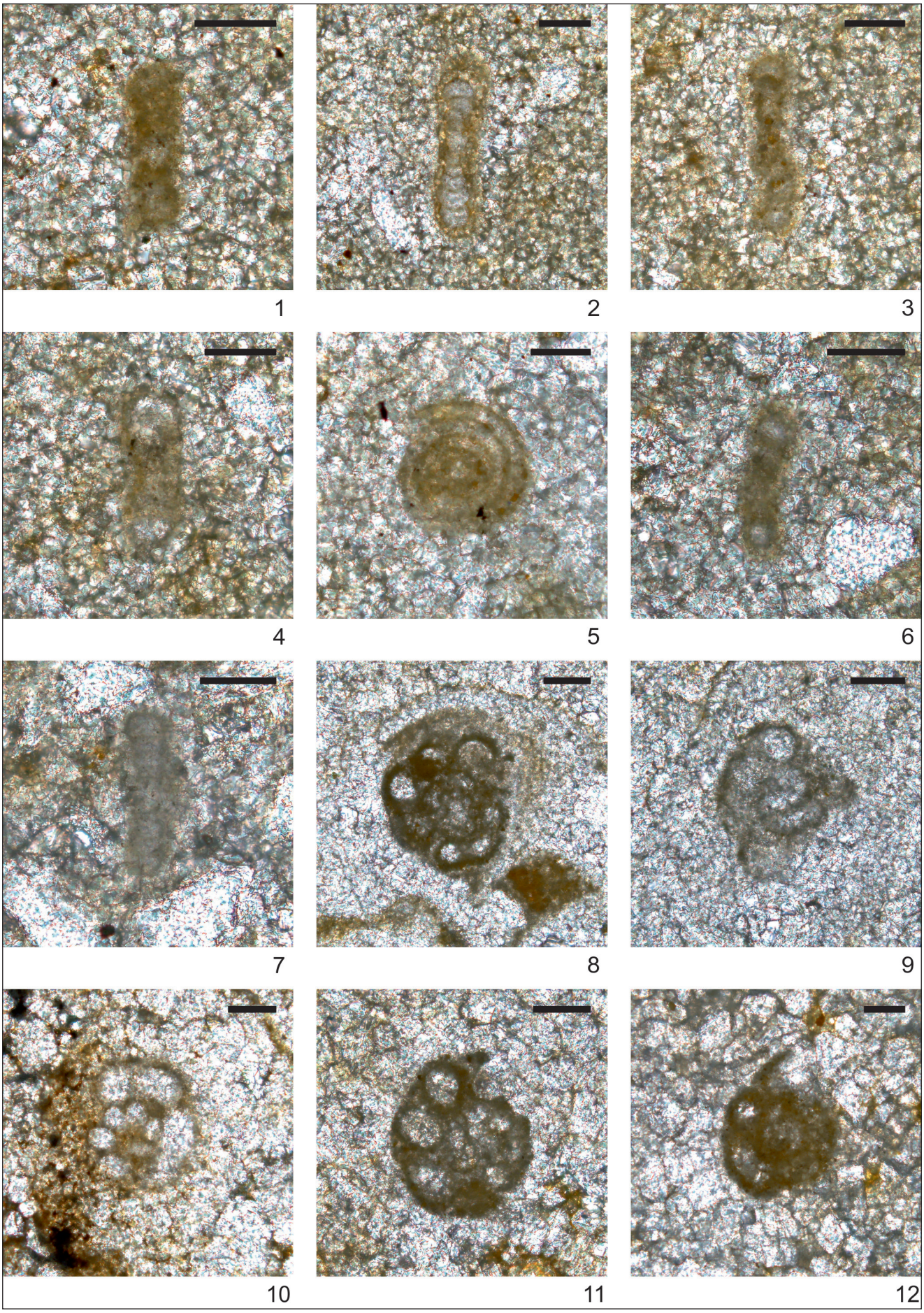
1
2
3
4
5
6
7
8
9
10
11
12

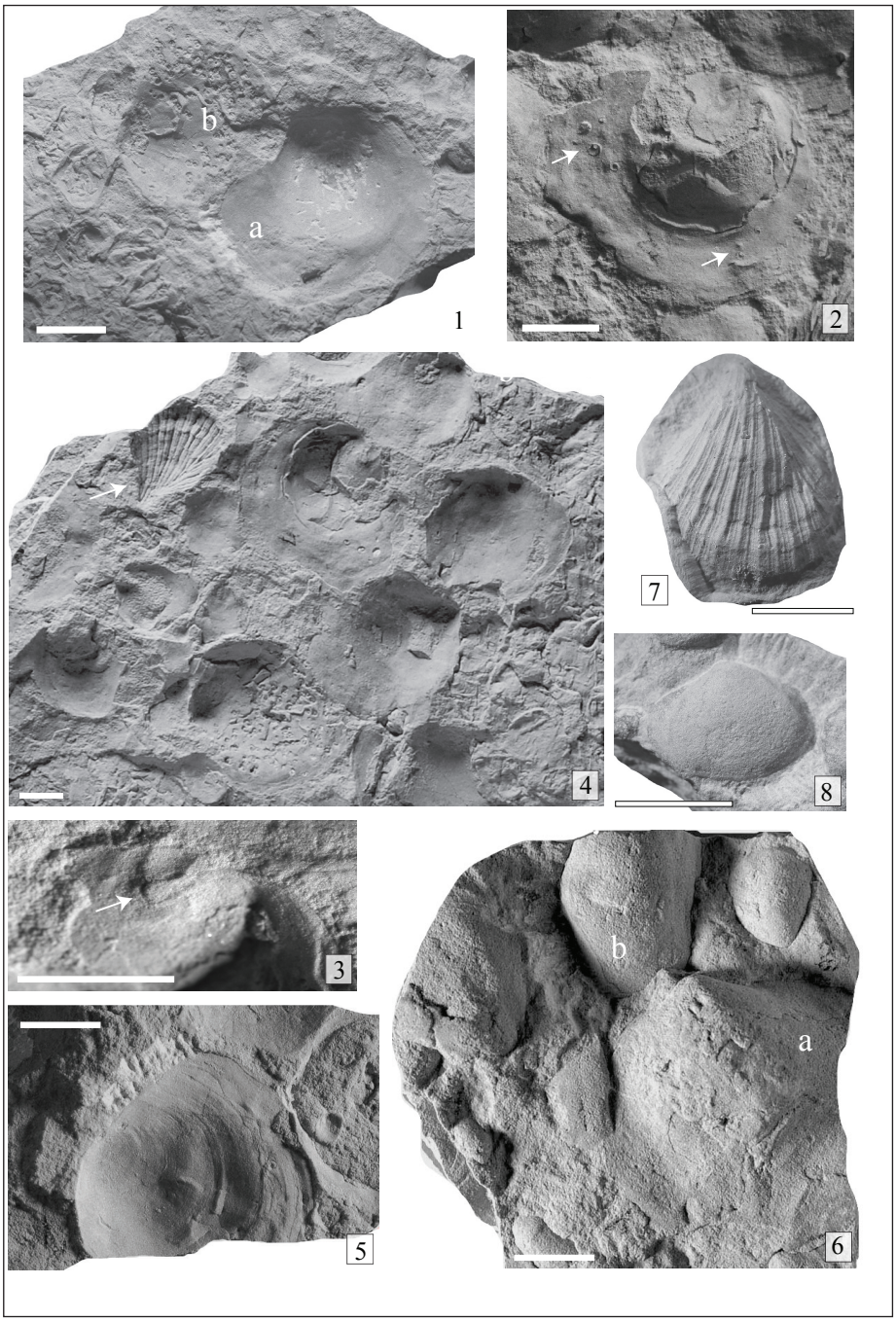

Fig. 16 - Bivalves from the Nimra Member (Ma'in Formation), Al Mamalih (Jordan).
1-6a) *Claraia bittneri* Ichikawa, 1958. 1a, external cast of left valve (specimen A1); 1b, external cast of left valve with weak radial ribs in the central part and microchonchid moulds on the posterior region (specimen A5). 2, 3, right valve with some encrusting microchonchids (arrows) and (3) detail of the umbonal depression and byssal notch (specimen A8). 4, shell pavement occurring on a lower bedding surface with the *Claraia*, *Unionites*? and *Eumorphotis* (arrow) assemblage. 5, external cast of a left valve (specimen C1); 6a, internal mould of a left valve (specimen B1).
6b) *Unionites*? sp., ? left valve.
7) *Eumorphotis multiformis* (Bittner, 1899), artificial mould of the left valve occurring on the bed surface of 4.
8) *Unionites*? *bittneri* (Frech, 1907), internal mould of a left valve (specimen D1). The scale bar is 10 mm.

Description. The shell is large (maximum length of 46 mm and 43 mm in hight), slightly retrocrescent, ovoid in outline and slightly longer than high (length/height ratio from 1.05 to 1.2). If compared to the most part of *Claraia* species, both valves are strongly inflated. The left valve inflation (T/H ratio) is about 20% of valve height, slightly greater than that of the right valve (12-15% of valve height). The left umbo extends slightly above hinge (Fig. 16, 6a) and is located one-third to two-fifths of the valve length behind the anterior margin. The left anterior ear is not detectable; the left posterior ear is undeveloped (Fig. 16, 1a). The right anterior ear is well defined and clearly separated from the disc (Fig. 16, 3). The byssal notch is deep and slightly oblique, with a keyhole shape (Fig. 16, 3). The right posterior ear is undeveloped. The right umbonal region shows a wide depression, which extends about one third of valve height (Fig. 16, 2). The valves are almost smooth. Irregular concentric lines and rare wrinkles are sometimes detectable along the marginal regions (Fig. 16, 2, 5). Radial ornaments have been observed in only one left valve (Fig. 15, 1b). They are barely detectable and represented by a few,

widely spaced and narrow costae occurring at the centre of the valve.

Discussion. The genus *Claraia* contains more than a hundred species and subspecies, which reflects an excessive taxonomical splitting (Newell & Boyd 1995), related to high genetic plasticity (Broglio Loriga et al. 1983), taxonomic provincialism (Assereto et al. 1973) and taphonomic bias. Therefore, the *Claraia* classification must be done applying a population-species concept (Posenato et al. 1996).

The *Claraia* population from Jordan belongs to the *Claraia aurita* group (Group 3 of Ichikawa 1958; Nakazawa 1977), the species of which are characterized by prevailing concentric ornamentation, represented by fine concentric lines and rare concentric folds; radial ribs are very weak or absent. The *C. aurita* group was divided by Nakazawa (1977) into two subgroups defined on the occurrence (3a) or absence (3b) of the posterior auricle. The here studied *Claraia* sample falls in the subgroup 3b, which contains the following species: *Claraia bittneri* Ichikawa, 1958, *Claraia griesbachi* (Bittner, 1899), *Claraia perthensis* Dickins & McTavish, 1963 and *Claraia zhenanica* Chen & Liu, 1964. The Jordanian *Claraia* differs from *C. zhenanica,* because the latter species has concentric and radial ornaments decidedly more developed (Chen & Liu in Gu et al. 1976, pl. 32, figs 7-8). *Claraia perthensis,* from western Australia, differs by the presence of a slight sinus along the posterior ear and a byssal notch "largely obsolete" at the adult stage (Dickins & McTavish 1963, pl. 1, figs 2-8). *Claraia griesbachi* has an almost flattened right valve and a byssal notch with subparallel or anteriorly divergent dorsal and ventral margins (Bittner 1899, pl. 1, figs 3, 4).

Claraia bittneri was proposed by Ichikawa (1958) to replace *Pseudomonotis tridentina* Bittner, 1901, an invalid species because of the occurrence of the senior homonym *Pseudomonotis tridentina* Tommasi, 1895 from the Middle Triassic Marmolada Limestone. *Claraia bittneri* was found in the Werfen Formation of Southern Alps (Val di Centa, Valsugana). The Jordanian species of *Claraia* and *C. bittneri* are characterized by the same ornamentation pattern, strong valve inflation, umbonal depression on the right valve, and a deep, obliquely oriented byssal notch represented by a narrow slit with parallel margins (Bittner 1901, pl. 24, fig. 3) or with a keyhole shape (Bittner 1901, pl. 24, fig. 2).

The ornamentation and outline of the Jordanian species of *Claraia* are also similar to *Claraia intermedia* Bittner, 1901, a species proposed on a syntype of *Posidonomya aurita* Hauer (Hauer 1850, pl. 3, fig. 6), which shows intermediate characters between *C. clarai* and *C. aurita*. However, all these three species are characterized by a left posterior auricle clearly separated from the disc (*C. aurita* subgroup 3a of Nakazawa 1977).

Considering the high intraspecific variability of *Claraia,* the great morphological affinities between the Jordanian population and the *C. bittneri* illustrated material, and the occurrence, among the figured *C. bittneri* syntypes, of a valve with an ovoid outline (Bittner 1901, pl. 24, fig. 5), the Jordanian population can be referred to *C. bittneri.*

Age. In the Iranian Elikah Formation, *Claraia aurita* is recorded in the *Gyronites* zone (lower Dienerian; Brühweiler et al. 2008), above *C. intermedia* and *C. radialis* beds (Nakazawa 1977). In the Werfen Formation of the Dolomites (Italy), *C. bittneri* is recorded within the *Claraia aurita* beds (Leonardi 1960), which corresponds to *Claraia aurita* group subzone (middle Siusi Member) representing the last Alpine *Claraia* subzone (Broglio Loriga et al. 1983, 1990). The upper boundary of the *Claraia aurita* group subzone corresponds to a $\delta^{13}C$ negative anomaly, which occurs at about 130 m above the base of Werfen Fm in the Bulla section, within the Dienerian *obliqua* Zone (Horacek et al. 2007; Foster et al. 2017). The lower boundary of the *C. aurita* group subzone corresponds to the disappearance of *C. clarai,* which subzone, corresponding to the lower Siusi Member, has been considered late Griesbachian – earliest Dienerian in age (Broglio Loriga et al. 1983). Therefore, *C. bittneri* suggests an early-middle Dienerian age.

Superfamily Heteropectinoidea Beurlen, 1954
Family Heteropectinidae Beurlen, 1954
Genus *Eumorphotis* Bittner, 1901
Type species *Pseudomonotis telleri* Bittner, 1898

Eumorphotis multiformis (Bittner, 1899)

Fig. 16, 7

*1899 *Pseudomonotis multiformis* Bittner, p. 10, pl. 2, figs 15–22.
1986 *Eumorphotis multiformis* (Bittner, 1899) - Broglio Loriga and Mirabella, p. 257-261, pl. 1, fig. 2.
2009 *Eumorphotis multiformis* (Bittner, 1899) - Kumagae & Nakazawa, p. 162, fig. 144.17 (with synonymies).
2014 *Eumorphotis multiformis* (Bittner, 1899) - Hoffmann et al., p. 18-19, fig. 11J-L.
* Only selected citations are reported.

Material and measurements: Only a left valve is available. It is represented both as external cast and internal mould with the anterior and posterior margins not completely preserved. The auricles are missing. The valve is about 23 mm long and 26 mm high.

Description. The left valve is moderately inflated, almost equilateral and with a pyriform outline. The umbo is probably orthogyrate; beak, hinge line and auricles not preserved. The ornamentation consists of numerous, slightly knobbed radial ribs of different order, increasing in number by intercalation. About 10 first-order ribs are irregularly intercalated by minor-order ribs. The rib formula, describing the intercalation order among the primary ribs (1, in bold), secondary ribs (2) and riblets (3,4) (e.g. Broglio Loriga & Miarabella 1986), observed along the central part of ventral region, is as follows: **1**, 4, 4, 2, 4, 3, 4, 4, **1**, 4, 4, 2, 4, 3, 4, **1**. The valve is also ornamented by fine growth lines and a deep commarginal growth break which occurs at about 5 mm from the ventral margin. Right valve and internal structure not present or observed.

Discussion. The pyriform outline and an ornamentation pattern characterized by only slightly knobbed, intercalated and multi-order radial ribs are typical of *Eumorphotis multiformis* (Bittner, 1899), a species characterized by a great morphological variability. This species and its varieties and synonymies have been described and discussed in detail by Broglio Loriga and Mirabella (1986). The species has a cosmopolitan distribution (e.g., Kumagae & Nakazawa 2009).

Age. *Eumorphotis multiformis* ranges from the lower Induan (Griesbachian) to lower Olenekian (Smithian). In the Dolomites it appears in the upper Griesbachian *Claraia clarai* subzone of the lower Siusi Member and disappears in the Gastropod Oolite Member (Broglio Loriga & Mirabella 1986), latest Dienerian – early Smithian in age (Posenato 2008a, b).

Order **Unionoida** Stolicza, 1871
Superfamily Anthracosioidea Amalitsky, 1892
Family Anthracosiidae Amalitsky, 1892
Genus *Unionites* Wissmann (in Münster), 1841
Type species: *Unionites muensteri* Wissmann (in Münster), 1841

Unionites*? *bittneri (Frech, 1907)

Fig. 16, 8

1901 *Myacites Fassaensis* Wiss. var. *brevis* Bittner, p. 84-85, pl. 9, figs 13-17.
1907 *Anoplophora Fassaensis* mut. *Bittneri* nov. nom. = mut. *brevis* Bittner, Frech, p. 41, pl. 7, fig. 1a, b.
1927 *Anodontophora (Myacites) fassaensis* Wissmann var. *Bittneri* Frech - Ogilvie Gordon, p. 27, pl. 2, fig. 27.
1927 *Anodontophora (Myacites) fassaensis* Wissmann var. *brevis* Bittner - Ogilvie Gordon, p. 27, pl. 2, fig. 26.
1935 *Homomya fassaensis* Wissm. var. *brevis* Bittner - Leonardi, 33-34, pl. 1, fig. 6.
1943 *Homomya fassaensis* Wissm. var. *brevis* Bittner - Boni, p. 4, pl. 1, fig. 17.

Material: A dozen of valves are available. They are preserved as internal moulds, outer casts and composite moulds. Diagenetic compression related to sediment compaction is low to absent. The preservation state does not allow us to observe many of the internal characters, such as the hinge structure and pallial line. Traces of the anterior muscle scar seem to be present in two specimens (A 15 and C 4).

Measurements (in mm) are presented in Tab. 7 and Fig. 17.

Description. The shell is small, slightly inequilateral, ovoid in outline and moderately inflated. The L/H ratio ranges from 1.23 to 1.37. The anterior margin is strongly rounded, broadly arched ventral margin. The posterior margin is almost truncated. The umbo is relatively broad, slightly prosogyrate and located at about 0.40 to 0.46 of valve length, behind the anterior margin. A rounded posterior carina extends from the beak to the posteroventral corner. The anterior muscle scar appears to be impressed; it originates an elevation on the internal mould (C4) or a depression on the internal valve surface (A15).

Discussion. The bivalve *"Myacites"* Auct. is very common in Lower Triassic formations, both in the Tethyian and Panthalassia regions. In the former region, the most common species are *"Myacites" fassaensis* Wissmann, 1841 and *"Tellina" canalensis* Catullo, 1846. Both these species have been created on material collected from the Werfen Formation of the Dolomites (northern Italy). The generic attribution of these species has been changed several times in the past (*Myacites, Anoplophora, Anodontophora, Pleuromya, Homomya, Unionites, Austrotindaria;* for the synonymies see Kumagae & Nakazawa 2009; Hautmann et al. 2013; Foster et al. 2016), because the type material does not preserve any internal taxonomical character. During the last decades, the most authors have followed the proposal of Ciriacks (1963), that classified the above cited species within *Unionites*. This generic classification has been recently questioned by Hautmann et al. (2013), while a different classification was proposed by Foster et

		Length	Height	LA	L/H
Unionites? fassaensis					
Wissmann 1841 lectotypus	**pl. 16, fig. 2a**	**33.00**	**21.00**	**12.00**	**1.57**
Hauer 1850	pl. 1, fig. 4a	27.00	17.00	12.00	1.59
	pl. 1, fig. 4b	25.00	15.00	12.00	1.67
Bittner 1899	pl. 3, fig. 28	19.00	12.00	6.00	1.58
	pl. 3, fig. 29	17.00	12.00	6.00	1.42
	pl. 3, fig. 30	16.00	10.50	5.00	1.52
	pl. 3, fig. 31	20.00	13.00	6.00	1.54
	pl. 3, fig. 32	20.00	12.00	7.00	1.67
	pl. 3, fig. 33	16.00	11.00	6.00	1.45
Wittenburg 1908	fig. 15	37.00	24.00	12.00	1.54
Ogilvie Gordon 1927	pl. 2, fig. 25a	29.00	19.00	12.00	1.53
Leonardi 1935	pl. 1, fig. 5	20.00	14.00	7.00	1.43
Newell & Kummel 1942	pl. 2, fig. 13	34.00	21.00	7.00	1.62
Ciriacks 1963	pl. 16, fig. 13	32.00	21.00	7.00	1.52
Unionites? bittneri					
Bittner 1901	pl. 9, fig. 13	8.50	6.50	3.00	1.31
	pl. 9, fig. 14	11.00	8.50	3.00	1.29
	pl. 9, fig. 15	11.50	9.00	3.50	1.28
	pl. 9, fig. 16	13.00	10.00	4.00	1.30
lectotypus	**pl. 9, fig. 17**	**28.50**	**23.00**	**7.00**	**1.24**
Frech 1907	pl. 7, fig. 1a	25.00	20.00	7.00	1.25
	pl. 7, fig. 1b	25.00	19.00	10.00	1.32
Ogilvie Gordon 1927	pl. 2, fig. 26	15.00	11.50	5.00	1.30
	pl. 2, fig. 27	18.00	14.00	7.00	1.29
Leonardi 1935	pl. 1, fig. 6	21.00	17.00	6.50	1.24
Neri & Posenato 1985	pl. 2, fig. 9	30.00	23.00	12.00	1.30
Jordan specimens	A3	15.10	12.30	6.50	1.23
	A4	8.20	6.50	3.60	1.26
	A15	10.40	7.60	4.20	1.37
	C4	19.50	14.60	9.00	1.34
	D1	21.80	15.90	10.00	1.37
	D3	14.70	10.90	5.90	1.35
	D4	19.10	14.30	7.80	1.34
	D6	13.30	10.00	5.30	1.33
	E2	27.20	21.80	11.70	1.25
	E3	9.60	7.80	4.00	1.23

Tab. 7 - Shell measurements for *Unionites*? *bittneri*.
The specimens from the literature, accepted here as reference for the species, have been measured on the author's figures from the literature; in bold, the here proposed lectotypes. Abbreviations: LA, distance of the umbo from the anterior margin. The measurements have been plotted in the scatter diagram of Fig. 17.

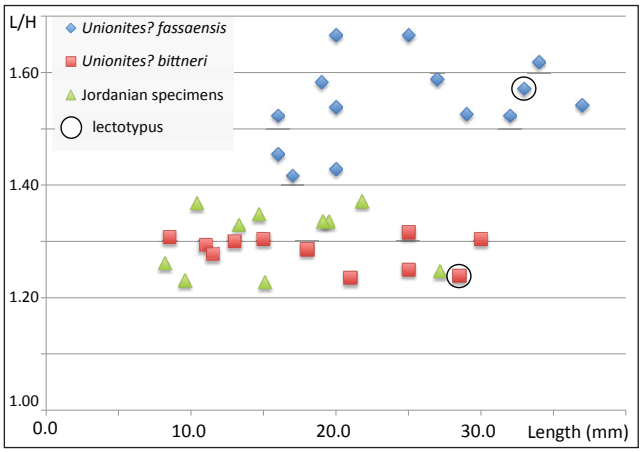

Fig. 17 - Scatter diagram of shell dimensions of *Unionites*? *fassaensis* (Wissmann), *Unionites*? *bittneri* (Frech) and *Unionites*? sp. from Jordan. The Jordanian population has a L/H ratio within the range of *Unionites*? *bittneri* (Frech).

al. (2016). The latter authors referred the majority of the past citations of *"Myacites" fassaensis* to the new species *Austrotindaria antiqua*. This classification is based on the finding of a taxodont hinge on silicified Lower Triassic bivalves from Svalbard and their supposed external similarities with specimens previously classified as *U. fassaensis*. However, the majority of the specimens from the Alps have an outline different from *Austrotindaria antiqua* (e.g., *A. antiqua* has a smaller and pointed beak). *"Myacites" fassaensis* has the priority on *A. antiqua* (e.g., the differences between the Wissmann syntypes and the specimens referred to *A. antiqua* have not been discussed), and the taxodont hinge has never been observed in the bivalves of the Werfen Formation. The generic classification of the Jordan material follows, therefore, the Hautmann et al. (2013) proposal. The occurrence of a deep anterior muscle scar, a taxonomical character of *Unionites muensteri* Wissmann (type species of *Unionites*) needs further confirmation to exclude its possible taphonomic origin.

The distinction between *Unionites*? *fassaensis* and *U.*? *canalensis* is sometimes difficult because they are characterized by a broad variability, related to population variability, taphonomic bias and inaccurate original diagnosis. *Unionites*? *canalensis* is characterized by an elongated and subrectangular outline, an umbo located at about two fifth of dorsal margin, a marked posterior carina and an almost straight ventral margin. In the Jordanian bivalves, an almost straight ventral margin occurs only in an incomplete left (?) valve, but the other characters are not detectable for the specimen incompleteness (Fig. 16, 6b).

Wissmann (in Münster 1841) figured three *"Myacites" fassaensis* syntypes (Wissmann in Münster 1841, pl. 14, fig. 2a-c), which show rather variable outlines. In the vague Wissmann's diagnosis, the species is characterized by an elongated ovoid outline, a large and sub-central umbo and an inclined posterior cardinal margin. The specimen of fig. 2a (Wissmann in Münster 1841, pl. 14) can be

considered the lectotype of *"M." fassaensis*, because Wissmann (in Münster 1841) described it as not deformed. It is a right valve with a rather elongated ovoid outline (L/H ratio of 1.65). The specimen of fig. 2c (considered as deformed by Wissmann in Münster 1841) is smaller and has a suborbicular outline (L/H ratio 1.08), while the specimen of fig. 2b is clearly deformed. *"Myacites" fassaensis* has been subsequently described and figured by many authors (see Kumagae & Nakazawa 2009 for a complete synonym list). The specimens included within this species have a L/H ratio mean of 1.5 (from 1.4 to 1.6; e.g., Hauer 1850; Bittner 1899; Wittenburg 1908; Ogilvie Gordon 1927; Leonardi 1935; Fig. 17).

The Jordanian specimens show affinities with the figured material of *"Myacites" fassaensis* (e.g., Wittenburg 1908; Ogilvie Gordon 1927; Leonardi 1935). However, the former has a lower L/H ratio, ranging from 1.23 to 1.37. The Jordanian "*Myacites"* have an ovoid outline shorter than the most part of the illustrated specimens of *"M." fassaensis*. A short ovoid outline characterizes *"Myacites" fassaensis* var. *brevis* Bittner 1901 from the Early Triassic of Tranasdanubian Mountain (Hungary). Frech (1907) noted that the Bittner's subspecies was a juvenile homonym of an Agassiz's species. Moreover, there is another *Unionites brevis* in literature. It is a species created by Schauroth (1857) on material from the Middle Triassic of Germany, which has a L/H ratio of 1.6. Frech (1907) replaced the name of Bittner's variety as follows: *Anoplophora fassaensis* mut. *bittneri* Frech, 1907.

The Jordanian specimens are not affected by relevant deformation, therefore their biometric values record a population variability without taphonomic bias. On the basis of the L/H ratio range lower (from 1.24 to 1.32) than that (from 1.42 to 1.67) of the specimens referred in the classical literature of the 19th and 20th centuries to *Unionites*? *fassaensis* this population is classified into the Frech's variety, here raised at specific level.

Age. *Unionites*? *brevis* has a wide stratigraphic distribution. In the Werfen Formation, it has been reported from the Induan *Claraia* Zone (Leonardi 1935) to the upper Olenekian *Dinarites* beds (Neri & Posenato 1985; Posenato 1992).

Palynology of the Umm Irna Formation

No new palynological data was obtained during the present study because organic-rich claystone beds that previously yielded palynomorphs and plant macro-flora from the Upper Permian Umm Irna Formation in the Dead Sea coastal exposures are absent in the Al Mamalih area. In summary, the palynological (Stephenson & Powell 2013, 2014) and plant macro-fossil data (Kerp et al. 2006; Abu Hamad et al. 2008) from the Dead Sea exposures including the common occurrence of the distinctive trisulcate pollen *Pretricolpipollenites bharadwaji* suggests an age range from latest Permian to Triassic for the Umm Irna Formation.

Discussion

Previous studies (Stephenson & Powell 2013; Powell et al. 2016) demonstrated that the Permian-Triassic (P-T) boundary in Jordan is marked by a major sequence boundary which is equivalent to Arabian Plate lowstand and overlying transgressive systems tract Tr 10 of Sharland et al. (2001, 2004). It separates the underlying alluvial plain lithofacies (Umm Irna Formation), of late Permian age, from the shallow marine lithofacies (Ma'in Formation) of Early Triassic age (Powell et al. 2016). These authors suggested that the constrained age of the section between the top of the Umm Irna Formation (based on palynomorphs and plant macro-flora) and the lowest limestone bed in the Nimra Member (Mai'n Formation) (based on conodonts and foraminifera) indicates that the section contains the Permian-Triassic boundary either within the hiatus represented by the sequence boundary or within the lower marine beds (i.e. the Himara Member and lowermost Nimra Member) above the sequence boundary. This stratigraphical interval, about 15 m thick, appears to span the most significant extinction event in the Phanerozoic (Wignall 2001; Benton & Twitchett 2003; Heydari & Hassanzadeh 2003). A latest Permian age based on the presence of abundant *Pretricolpipollenites bharadwaji* has been determined for the uppermost alluvial plain sediments preserved immediately below the sequence boundary (Stephenson & Powell 2013, 2014). Powell et al. (2016) demonstrated the presence of conodonts (e.g. *Hadrodontina aequabilis*) and foraminifera (e.g. *"Cornuspira" mahajeri*) from thin wackestones in the lower Nimra Member exposed near the Dead Sea shore, that indicated an Early Triassic (Induan) age for the Nimra Member.

Coeval Upper Permian to Lower Triassic rocks were first described earlier (Powell & Moh'd 1993) from the Al Mamalih area located about 7 km inland and to the south-east of the Dead Sea sections, but their precise age was not known. Re-sampling of the limestones from the previously reported Dead Sea sections and detailed logging and sampling of the Al Mamalih sections has revealed an abundant, but low diversity fauna of conodonts, bivalves and foraminifera from the Lower Triassic beds. Abundant elements of the conodont apparatus have allowed a better understanding of the morphology of the key taxa *Hadrodontina aequabilis* Staesche, 1964 and *Hadrodontina agordina* (Perri & Andraghetti 1987). These species are known to have favoured shallow water environments and were euryhaline, thus tolerant of restricted marine environments. Similarly, the wackestones yielded a low diversity foraminifera assemblage from the Nimra Member in the Al Mamalih sections, represented by the new species *Ammodiscus jordanensis*. This taxon together with *"Cornuspira" mahajeri* reported previously from the Dead Sea sections (Powell et al. 2016) is also interpreted as opportunistic 'disaster species' (Groves et al. 2005) characteristic of the survival phase after the latest Permian mass extinction event. Other disaster taxa are represented by the bivalves *Claraia, Eumorphotis* and *Unionites*, which dominate the shallow benthic marine communities throughout Tethys and Panthalassa realms. These bivalves thrived mostly during the Induan, in the aftermath of the end Permian extinction (Hallam & Wignall 1997). The presence of low angle cross-stratification in the limestones together with crinoid, echinoid, gastropods fragments, abraded fragments of conodonts and glauconitic/phosphatic peloids further indicate a high energy, shallow water depositional environment.

The red/mauve Himara Member (Figs 7, 8, 9), above the sequence boundary, is faunally barren except for sparse, surface trace fossils in ripple-marked siltstones and fine-grained sandstones (Fig. 9b). Wave ripples and desiccation cracks indicate a shallow water setting and temporary emergence. Red colouration may be due to reworking of the underlying Umm Irna alluvial red-beds rather than primary oxidative reddening. Sedimentary structures, trace fossils and macro/micro-fauna indicate a shallow, restricted marine environment. Following the initial marine transgression in Early Triassic (Induan) time the shallow marine environment became increasingly conducive to shallow marine faunas (high abundance/low diversity bivalves and conchostracans) with opportunistic colonisation of substrates (surface burrows). Foraminifera and conodonts as well as fragmental echinoderms, marine bivalves (e.g., *Claraia* and *Eumorphotis*), gastropods and tubeworms (microchonchids), as well as stromatolites indicate the establishment of shallow marine conditions during deposition of the Nimra Member.

The limestone beds of the Nimra Member can be correlated over 7 km between the Al Mamalih area and the Dead Sea outcrops located to the west, but they wedge-out northwards from these outcrops indicating that these shallow-water carbonate environments were present only at the southern margin of the basin during Induan times.

The precise timing of events over Permian (Umm Irna Formation) to Triassic (Ma'in Formation) transition in the Levant is still the subject of debate. Palynological data indicate a latest Permian age for the uppermost Umm Irna Formation based on the presence of abundant *Pretricolpipollenites bharadwajii* (Stephenson & Powell 2013, 2014). Furthermore, Powell et al. (2016) demonstrated the presence of conodonts (e.g. *Hadrodontina aequabilis*) and foraminifera (e.g. "*Cornuspira*" *mahajeri*) from the limestones in the lower Nimra Member exposed near the Dead Sea shore, that indicated an Early Triassic (Induan) age for the Nimra Member. The current study of the Al Mamalih sections adds the discovery of a middle Induan *Claraia* species to our knowledge of the biostratigraphically significant conodont/foraminifera and bivalves and confirms the age of the lower Nimra Member (*ca* 15 m above the sequence boundary) as equivalent to the beds above the *isarcica* Zone in the Southern Alps where *Hadrodontina aequabilis* and *Hd. agordina* co-exist within and above the stratigraphic range of *Hindeodus postparvus*, that is, mid Induan. The presence of the new foraminifera species *Ammodiscus jordanensis* n. sp. in samples AN 14 (Section 1) and AN 20 (Section 2) is also thought to be Induan in age because these samples are correlated with the similar carbonate beds of the Dyke Plateau/Roadside sections near the Dead Sea which are considered Induan in age on the basis of the *P.* gr. *kalhori-Earlandia* spp. assemblage (Powell et al. 2016).

Sample AN 31, of the stratigraphically higher Upper Carbonate Member (Dardun Formation) in the Panorama Road section, records, the FO of

Citaella pusilla (Ho, 1959), also present in AN 32. Since the foraminifera assemblage *Postcladella* gr. *kahlori-Earlandia* spp.-*Ammodiscus jordanensis* n. sp. is considered as Induan in age, whilst *Citaella pusilla* is typical of the Olenekian (Broglio Loriga et al. 1990; Rettori 1995), the stratigraphic interval, from sample AN 29 to AN 32 of the Upper Carbonate Member (Dardun Formation), spans the Induan-Olenekian boundary interval.

The Umm Irna-Ma'in sequence boundary was interpreted by Powell et al. (2016) as equivalent to the Tr 10 Arabian Plate unconformity taken at the base of the Khartam Member of the Kuff Formation in the Unayzah area of central Saudi Arabia (Sharland et al. 2004), and in the subsurface near the top of Kuff B (Le Nindre et al. 1990). At outcrop in the Unayzah area, the Triassic marine flooding event (Tr 10) is similarly marked by marine shales with an open marine fauna, overlying channelized fluvial sandstones with plant remains (Sharland et al. 2004, fig. 4.32). This suggests a widespread and rapid transgression across the low topographical gradient of the Arabian Plate in early Induan times, a response to rapidly rising sea-levels.

Basinwards, in the Negev area and below the present-day coastal plain of Israel, deep boreholes (Avdat 1, Pleshet 1 and David 1) proved proximal to distal marine siliciclastic and carbonate successions spanning the Permian to Triassic transition (Hirsch 1975, 1992; Korngreen et al. 2013; Korngreen & Zilberman 2017). Here, the strata are characterised by distal siliciclastic and ramp carbonates. Avdat 1 represents the most proximal succession and the Upper Permian interval is considered here to be coeval with the lower part of the Dead Sea/Al Mamalih succession (Umm Irna Formation), the latter representing deposition in coeval alluvial environments in the hinterland (Stephenson & Powell 2013). Reconstruction of the locations of the Maktesh Qatan 2 and Avdat 1 boreholes in the Negev (Hirsch 1975; Korngreen et al. 2013) to take account of *ca* 105 km left-lateral movement along the Dead Sea Transform (Freund et al. 1970) places these successions about 50 km to the north and northwest, respectively, of the Al Mamalih outcrops. This suggests a relatively rapid basinward transition during the latest Permian, from a low-gradient alluvial coastal plain (Jordan) with high sinuosity and meandering rivers to shallow marine environments (Israel). In Jordan, the transgressive marine environment appears to have been established in earliest Triassic time (probably early Induan = Himara Member) when rapid sea-level rise resulted in the initial marine flooding of the Arabian Plate. Previously, it has been suggested that the boundary between the Upper Permian Umm Irna and Lower Triassic Ma'in formations, represents a hiatus (Stephenson & Powell 2013; Powell et al. 2016). However, the basal unit, the Himara Member has not yielded biostratigraphically useful fauna or flora and may represent the post-recovery interval above the P-T boundary when biota was sparse due to stressed environments. Consequently, the upper part of the Umm Irna Formation may be indeed latest Permian in age, equivalent to the shallow marine strata proved basinwards in the boreholes (Israel), with the sequence boundary (Jordan) representing the P-T boundary which is known to be a short interval of low $\delta^{13}C_{org}$ (Korngreen & Zilberman 2017) followed by a faunally barren Himara Member.

Powell et al. (2016) suggested that the lithofacies, faunas and biostratigraphy indicate the Himara Member, above the sequence boundary, represents a recovering marine phase and progressive transgressional systems tract that post-dates the P-T extinction event. The paleoclimate during deposition of the uppermost Umm Irna Formation (Late Permian) was humid-tropical, but with seasonal fluvial discharge and a fluctuating groundwater regime resulting in highly evolved pisolitic ferruginous paleosols on the interfluves. Fluvial systems evolved through time from low- to high-sinuosity rivers where in the latter organic material and macro-plants were preserved on point bars within channels (Makhlouf et al. 1991; Abu Hamad et al. 2008; Stephenson & Powell 2013). However, in contrast to the Dead Sea outcrops, the Umm Irna Formation in the Al Mamalih area is devoid of the organic-rich, laterally-accreted point-bar deposits that yielded abundant, well-preserved macrofossils at Dyke Plateau. Although separated by only 7 km, this suggests a higher energy fluvial regime in the Al Mamalih area with deposition predominantly by low sinuosity rivers, compared to a lower energy meandering regime preserved in the uppermost part of the Umm Irna Formation of the Dead Sea outcrops. Clearly, the fluvial systems suggest there was a fluctuating climate regime during the late Permian in the region. A warm, arid climate during the early Triassic in this region is also supported by reddening (perhaps secondary in origin) and desiccation features in the

shallow marine Himara Member and the presence of shallow water carbonates in the Nimra Member, adding to isotope evidence, such as $\delta^{18}O$ profiles (Korngreen & Zilberman 2017), for the region lying about 15 to 20 degrees south of the paleo-equator at the northern margin of the Arabian Plate during a period of global warming through the Permian to Triassic transition (Stampfli & Borel 2002; Korngreen & Zilberman 2017).

Conclusions

The Al Mamalih outcrops represent the Late Permian to Early Triassic transition and confirm that the Permian-Triassic boundary is constrained either within the hiatus represented by the sequence boundary between the alluvial Umm Irna Formation and the overlying shallow marine Ma'in Formation, or within ca 15 m of marine beds overlying the boundary (Himara Member). The sequence boundary can be traced over a wide area and the absence of a paleotopography immediately below the boundary suggests that the marine transgression advanced rapidly across a low-lying coastal/alluvial plain. Alluvial lithofacies (Jordan) passed basinwards, over a distance of about 50 km, to coeval shallow marine siliciclastic and carbonate environments proved in boreholes in the Negev and Mediterranean coast of Israel.

The Al Mamalih outcrops are preserved in pre-Cretaceous paleograbens bounded by late Jurassic extensional faults so that the outcrops are not contiguous. However, detailed logging allows correlation between the paleograbens and Dead Sea outcrops. Reddened, shallow-marine beds characterised by ripple cross-laminated, siltstone/sandstone with desiccation cracks and sparse surface burrows mark the initial Triassic (presumed early Induan) marine transgression (Himara Member) above the sequence boundary. Absence of both body fossils and vertical infaunal burrows reflects low-diversity, ecosystems following the Permian-Triassic extinction event, and/or because of stressed shallow marine environments. A gradational upward increase in grey, green and yellow siltstones beds (Nimra Member) accompanied by a concomitant increase in bioturbation (surface traces and infaunal vertical burrows), decalcified bivalves, stromatolites, conchostracans and lingulids in the lower part of the Nimra Member indicates colonisation of the substrate under shallow marine conditions during the recovery phase following the P-T extinction event. A high energy, shallow-water marine environment is indicated by the presence of two thin limestone (packstone) beds with shallow scours and bivalve lags with shell fragments of the newly described *Claraia*, in the Dead Sea outcrops and coeval wake- packstones and sandy limestones in the Al Mamalih area.

The carbonate-rich lithologies in the Nimra Member yielded an abundant, low diversity assemblage of conodonts (e.g. *Hadrodontina aequabilis* and *Hd. agordina*) and a foraminifera assemblage (*Postcladella* gr. *kalhori-Earlandia* spp.-*Ammodiscus jordanensis* n. sp.) that are interpreted as euryhaline recovery taxa that characterize the Induan. Abundant new material has allowed revision of the conodont apparatus of the taxa, and the foraminifera include a new species *Ammodiscus jordanensis* n. sp. of Induan age. The lithofacies and faunas are similar to the Lower Triassic Werfen Formation of the Southern Alps, suggesting post-extinction recovery sediments were deposited over a wide area on the northern and southern margins of Paleo-Tethys. This Early Triassic marine transgression (Tr 10 of Sharland et al. 2004) can also be traced widely eastwards across the Arabian Plate where overlying thick carbonates (Khuff Formation) represent one of the world's most prolific hydrocarbons reservoirs.

A humid-tropical climate during the Permian to Triassic transition is suggested by the presence of highly evolved paleosols (interfluves) and abundant macro-plant fossils as well as palynomorphs preserved within high-sinuosity channels in the uppermost Permian sediments near the Dead Sea, and the presence of reddened, ripple marked siliciclastics with desiccation cracks in the earliest Triassic sediments. Carbonate faunas in the overlying beds also point to a warm, shallow sea during the Induan recovery phase.

Acknowledgements: We thank Simon Ward and Ian Longhurst for preparing the figures. John Powell and Mike Stephenson publish with the permission of the Executive Director, British Geological Survey (NERC). The authors thank the anonymous reviewers for their helpful comments and suggestions. We acknowledge Agostino Rizzi for photos at SEM, CNR Dipartimento di Scienze della Terra "Ardito Desio". We are grateful to the Department of Earth Sciences "Ardito Desio", University of Milano and the University of Ferrara for financial support.

References

Abu Hamad A., Kerp H., Vording B. & Bandel K. (2008) - A Late Permian flora with *Dicroidium* from the Dead Sea region, Jordan. *Rev. Palaeobot. Palynol.,* 149: 85-130.

Assereto R., Bosellini A., Fantini Sestini N. & Sweet W. C. (1973) - The Permian–Triassic boundary in the Southern Alps (Italy): 176-199. In: A. Logan and L. V. Hill (Eds) - Permian and Triassic Systems and their Mutual Boundary Memoirs, vol. 2. *Canad. Soc. Petrol. Geol.*, Calgary.

Alsharhan A.S. & Nairn A.E.M. (1997) - Sedimentary Basins and Petroleum Geology of the Middle East. Elsevier, Amsterdam, 843 pp.

Altıner D., Baud A., Guex J. & Stampfli G. (1980) - La limite Permien–Trias dans quelques localités du Moyen-Orient: recherches stratigraphiques et micropaléontologiques. *Riv. It. Paleontol. Strat.* 85: 683-714.

Altıner D. & Zaninetti L. (1981) - Le Trias dans la région de Pinarbasi, Taurus oriental, Turquie: unités lithologiques, micropaleontologie, milieux de dépôt. *Riv. It. Paleontol. Strat.,* 86: 705-60.

Bandel K. & Khoury H. (1981) - Lithostratigraphy of the Triassic in Jordan. *Facies*, 4: 126.

Bender F. (1974) - Geology of Jordan, Gebruder Borntraeger, Berlin, 196 pp.

Benton M.J. & Twitchett R.J. (2003) - How to kill (almost) all life: the end Permian extinction event. *Trends Ecol. Evol.*, 18: 358-365.

Bittner A. (1899) - Trias Brachiopoda and Lamellibranchiata. *Palaeont. Indica,* Ser. 15, Himalayan Fossils, 3(2): 1-76.

Bittner A. (1901) - Ueber *Pseudomonotis Telleri* und verwandte Arten der unterer Trias. *Jarh. k.-k.Geol. Reich.,* 50(4): 559-593.

Boni A. (1943) - Revisione della Fauna triassica bresciana: la fauna del Trias Inferiore. *Riv. It. Paleontol. Strat.,* 49(2): 1-40.

Broglio Loriga C. & Mirabella S. (1986) - Il genere *Eumorphotis* Bitter, 1901 nella biostratigrafia dello Scitico, Formazione di Werfen. *Mem. Sci. Geol. Padova,* 38, 245-281.

Broglio Loriga C., Masetti D. & Neri C. (1983) - La Formazione di Werfen (Scitico) delle Dolomiti occidentali. *Riv. It. Paleontol. Strat.,* 88(4): 501-598.

Broglio Loriga C., Goczan F., Haas J., Lenner K., Neri C., Oravecz Sheffer A., Posenato R., Szabo I. & Toth Makk A. (1990) - The Lower Triassic sequences of the Dolomites (Italy) and Transdanubian Mid-Mountains (Hungary) and their correlation. *Mem. Sci. Geol. Padova,* 42: 41-103.

Brosse M., Bucher H., Bagherpour B., Baud A., Frisk A.M., Guodun K. & Goudemand N. (2015) - Conodonts from the Early Triassic microbialite of Guangxi (South China): Implications for the definition of the base of the Triassic System. *Palaeontology*, 2015: 1-22.

Brühweiler T., Brayard A., Bucher H. & Goudun K. (2008) - Griesbachian and Dienerian (Early Triassic) ammonoid faunas from northwestern Guangxi and southern Guizhou (south China). *Palaeontology,* 51(5): 1151-1180.

Carter J.C., Altaba C.R., Anderson L.C., Araujo R., Biakov A.S., Bogan A.E. et al. (2011) - A synoptical classification of the Bivalvia (Mollusca). *Paleontol. Contr.,* 4: 1-47.

Chen J., Beatty T.W., Henderson C.M. & Rowe H. (2009) - Conodont biostratigraphy across the Permian–Triassic boundary at the Dawen section, Great Bank of Guizhou, Guizhou Province, South China: implications for the Late Permian extinction and correlation with Meishan. *J. Asian Earth. Sci.*, 36(6): 442-458.

Ciriacks K. W. (1963) - Permian and Eotriassic bivalves of the Middle Rockies. *Bull. Am. Mus. Nat. Hist.,* 125(1): 1-100.

Cox L.R. (1924) - Triassic fauna from the Jordan valley. *Ann. Mag. Nat. Hist. Mus., London,* 14: 5296.

Cox L.R. (1932) - Further notes on the Transjordan Trias. *Ann. Mag. Nat. Hist. Mus. London*, 10: 93113.

Dai J.Y. & Zhang J.H. (1989) - Conodonts. In: Li Z.S., Zhan L.P., Dai J.Y., Jin R.G., Zhu X.F., Zhang J.H., Huang H.Q., Xu D.Y., Yan Z. & Li H.M. (Eds) - Study on the Permian–Triassic Biostratigraphy and Event Stratigraphy of Northern Sichuan and Southern Shaanxi. Ministry of Geology and Mineral Resources, Geological Memoirs, Series 2, 9: 428-435, Geological Publishing House, Beijing.

Dickins J.M. & McTavish R.A. (1963) - Lower Triassic marine fossils from the Beagle Ridge (BMR 10) Bore, Perth Basin, Western Australia. *J. Geol. Soc. Australia*, 10(1): 123-140.

Dill H.G., Bechtel A., Jus J., Gratzer R. & Abu Hamad A.M.B. (2010) - Deposition and alteration of carbonaceous series within a Neotethyan rift at the western boundary of the Arabian Plate: The Late Permian Umm Irna Formation, NW Jordan, a petroleum system. *Intern. J. Coal Geol.*, 81: 1-24.

Donoghue P.C.J., Purnell M.A., Aldridge R.J. & Zhang S. (2008) - The interrelationships of 'complex' conodonts (Vertebrata). *J. System. Palaeontol.,* 6: 119-153.

Epstein A.G., Epstein J.B. & Harris D.L. (1977) - Conodont Colouration Alteration – An Index to Organic Metamorphism. *Professional Paper, U.S. Geol. Surv.*, 995 pp.

Eshet Y. (1990) - Paleozoic-Mesozoic palynology of Israel, I. Palynological aspects of the Permo-Triassic succession in the subsurface. *Geol. Surv. Israel Bull.*, 81: 1-20.

Eshet Y. & Cousminer H. L. (1986) - Palynozonation and correlation of the Permo-Triassic succession in the Negev, Israel. *Micropaleontol.*, 32: 193-214.

Farabegoli E. & Perri M.C. (1998) - Permian/Triassic boundary and Early Triassic of the Bulla section (Southern Alps, Italy): lithostratigraphy, facies and conodont biostratigraphy. In: M.C. Perri & C. Spalletta (Eds) - Southern Alps Field Trip Guidebook, ECOS VII. *Giornale di Geologia*, 60, Spec. Issue: 292-310.

Farabegoli E. & Perri M.C. (2012) - Millennial physical events and the end-Permian mass mortality in the western Palaeotethys: timing and primary causes, In: Talent J.A. (Ed.) - Earth and Life: 719-758. Extinction Intervals and Biogeographic Perturbations through Time, International Year of Planet Earth. DOI10.1007/978-90-481-

3428-1_24, Springer Science +Business Media B.V.2012, Dordrecht.

Farabegoli E. Perri M.C. & Posenato R. (2007) - Environmental and biotic changes across the Permian–Triassic boundary in western Tethys: The Bulla parastratotype, Italy. *Global Planet. Changes,* 55: 109-135.

Fischer A.G. & Arthur M.A. (1977) - Secular variations in the pelagic realm. In: Cook H.E. & Enos P. (Eds) - Deep-water carbonate environments, Spec. Publ. 25: 19-50. *Soc. Econ. Paleontol. Mineral.*, Los Angeles.

Foster W.J., Danise S.D. & Twitchett R.J. (2016) - A silicified Early Triassic marine assemblage from Svalbard. *J. Syst. Palaeontol.,* 15(10): 851-877.

Foster W.J., Danise S.D., Price G.D. & Twitchett R.J. (2017) - Subsequent biotic crises delayed marine recovery following the late Permian mass extinction event in northern Italy. *PloseOne* 12(3): e0172321.

Frech F. (1907) - Die Leifossilien der Werfener Schichten und Nachträge zur Fauna des Muschelkalkes der Cassianer Schichten sowie des Rhaet und des Dachsteindolomites (Hauotdolomit). *Res. wiss. Erforsch. Balatonsees*, I(1), *Pal. Anh.*, 95 pp.

Freund R.Z., Garfunkel Z., Zak I, Goldberg M., Weissbrod T. & Derin B. (1970) - The shear along the Dead Sea rift. *Phil. Trans. Royal Soc. London*, A.267: 107-130.

Groves J.R., Altıner D. & Rettori R. (2005) - Extinction, survival, and recovery of lagenide foraminifers in the Permian–Triassic boundary interval, Central Taurides, Turkey. *J. Paleontol.*, 79 (suppl.): 1-38.

Groves J.R., Rettori R., Payne J.L., Boyce M.D. & Altiner D. (2007) - End-Permian mass extinction of lagenide foraminifers in the Southern Alps (Northern Italy). *J. Paleontol.*, 81: 415-34.

Gu Z.W., Huang B.Y., Chen C.Z. & Wen S.X. (1976) - Fossil Lamellibranchiata of China. Science Press, Beijing, 522 pp. (in Chinese).

Hallam A. & Wignall P.B. (1997) - Mass extinction and their aftermath. Oxford University Press, 320 pp.

Hauer F. von (1850) - Ueber die vom Herrn Bergrat W. Fuchs in den Venetianer Alpen gesammelten Fossilien. *Denksch. k. Ak. Wiss. Wien, Mat.-Natur. Kl.,* 2: 1-19.

Hautmann M., Smith A.B., McGowan A.J. & Bucher H. (2013) - Bivalves from the Olenekian (Early Triassic) of south-western Utah: systematics and evolutionary significance. *J. Syst. Palaeontol.*, 11(3): 263-293.

He W., Feng Q., Weldon E.A., Gu S., Meng S., Zhang F. & Wu S. (2007) - A Late Permian to Early Triassic Bivalve Fauna from the Dongpan Section Southern Guangxi, South China. *J. Paleontol.,* 81(5): 1009-1019.

He L., Wang Y., Woods A., Li G., Yang H. & Liao W. (2012) - Calcareous tubeworms as disaster forms after the end-Permian mass extinction In South China. *Palaios*, 27: 878-886.

Heydari E. & Hassanzadeh J. (2003) - Deev Jahni model of the Permian-Triassic boundary mass extinction: a case for gas hydrates as the main cause of biological crisis on Earth. *Sedim. Geol.*, 163: 147-163.

Hirsch F. (1975) - Lower Triassic conodonts from Israel. *Bulletin* 66: 39-46. Geol. Surv. Israel.

Hirsch, F. (1992) - Circummediterranean Triasic eustatic cycles. *Isr. J. Earth Sci.*, 40: 29-38.

Ho Y. (1959) - Triassic Foraminifera from the Chialingkiang Limestone of South Szechuan. *Acta Paleont. Sinica*, 7: 387-418.

Horacek M., Brandner R. & Abart R. (2007) - Carbon isotope record of the P/T boundary and the Lower Triassic in the Southern Alps: evidences for rapid changes in storage of organic carbon. *Palaeogeogr., Palaeoclimatol., Palaeoecol.,* 252: 347-354.

Huckriede R. (1958) - Die conodonten der mediterranen Trias und ihr stratigraphischer Wert. *Paläontol. Z.,* 32: 141-175.

Ichikawa K. (1958) - Zur taxionomie und Phylogenie der Triadischen "Pteriidae" (Lamellibranch.). *Palaeontographica,* A, 111: 131-212.

Jablonski D. (2002) - Survival without recovery after mass extinctions. *PNAS,* 99 (12): 8139-8144.

Jiang H. S., Lai X.L., Sun Y.D., Wignall P.B., Liu J. & Yan C. (2014) - Permian–Triassic Conodonts from Dajiang (Guizhou, South China) and Their Implication for the Age of Microbialite Deposition in the Aftermath of the End-Permian Mass Extinction. *J. Earth Sci.*, 25(3): 413-430, doi:10.1007/s12583-014-0444-4.

Kaim A. & Nützel A. (2011) - Dead bellerophontids walking - The short Mesozoic history of the Bellerophontoidea (Gastropoda). *Palaeogeogr., Palaeoclimatol., Palaeoecol.,* 308 (1-2): 190-199.

Kerp H., Abu Hamad A., Vörding B. & Bandel K. (2006) - Typical Triassic Gondwana floral elements in the Upper Permian of the paleotropics. *Geology*, 34: 265-268.

Koike T. (2016) - Multielement conodont apparatuses of the Ellisonidae from Japan. *Paleontol. Res.*, 20(3): 161-175.

Koike T., Yamakita S. & Kadota N. (2004) - A natural assemblage of *Ellisonia* sp. cf. *E. triassica* Müller (Vertebrata: Conodonta) from the uppermost Permian in the Suzuka Mountains, central Japan. *Paleontol. Res.*, 8: 241-253.

Kolar-Jurkovšek T., Jurkovšek B. & Aljinovic D. (2011) - Conodont biostratigraphy and lithostratigraphy across the Permian–Triassic boundary at the Lukac section in western Slovenia. *Riv. It. Paleontol. Strat.*, 117: 115-133.

Korngreen D., Orlov-Labkovsky O., Bialik O. & Benjamini C. (2013) - The Permian-Triassic transition in the central coastal plain of Israel (North Arabian Plate margin), David 1 Borehole. *Palaios*, 28: 491-508.

Korngreen D. & Zilberman T. (2017) - The role of land-marine teleconnections in the tropical proximal Permian-Triassic Marine Zone, Levant Basin, Israel: Insights from stable isotope pairing. *Global Plan. Change,* 154: 44–60.

Kozur H. (1977) - Revision der Conodontengattung *Anchignathodus* und ihrer Typusart. *Zeit. geol. Wiss.,* 5(9): 1113-1127.

Kozur H. (1990) - Significance of events in conodont evolution for the Permian and Triassic stratigraphy. *Courier Forschung. Senckenberg*, 117: 385-408.

Kozur H. (1996) - The conodonts *Hindeodus*, *Isarcicella* and *Sweetohindeodus* in the Uppermost Permian and Lower-

most Triassic. *Geol. Croatica*, 49: 8l-115, Zagreb.

Krainer K., Vachard D. & Lucas S.G. (2005) - Lithostratigraphy and biostratigraphy of the Pennsylvanian-Permian transition in the Jemez Mountains, North-Central New Mexico. In: Lucas S.G., Zeigler K.E. & Spielmann J.A. (Eds) - The Permian of Central New Mexico, Bulletin 31: 74-89. Mus. Nat. Hist. Sci., New Mexico.

Kumagae T. & Nakazawa K. (2009) - Bivalves. In: Shigeta Y., Zakharov, Y.D., Maeda H. & Popov A.M (Eds) - The Lower Triassic System in the Abrek Bay area, South Primorye, Russia. National Museum Nature Science Monographs, Tokyo, 38: 156-173.

Le Nindre Y.M, Vaslet D. & Manivit J. (1990) - Le Permo-Trias d'Arabie Centrale. *Documents de BRGM*, 193: 1-559.

Leonardi P. (1935) - Il Trias Inferiore delle Venezie. *Mem. Sci. Geol. Padova,* 11: 1-136.

Leonardi P. (1960) - Studio statistico-sedimentologico di alcune faune werfeniane della Valle di Fiemme nel Trentino. *St. Trent. Sc. Nat.*, 37: 17-29.

Lyu Z., Orchard M.J., Chen Z., Wang X., Zhao L. & Chen H. (2017) - Uppermost Permian to Lower Triassic conodont successions from the Enshi area, western Hubei Province, South China. *Palaeogeogr., Palaeoclimatol., Palaeoecol.*, DOI: 10.1016/jpalaeo.2017.08.015.

Makhlouf I. M. (1987) - The stratigraphy and sedimentation of Upper Cambrian, PermoTriassic and Lower Triassic rocks along the northeastern margin of the Dead Sea basin, Jordan. Unpublished Ph. D thesis, University of Newcastle upon Tyne, U.K.

Makhlouf I. M., Turner B.R. & Abed A.M. (1991) - Depositional facies and environments in the Permian Umm Irna Formation, Dead Sea area, Jordan. *Sedim. Geol.*, 73: 117-139.

Metcalfe I. (1995) - Mixed Permo-Triassic boundary conodont assemblages from Gua Sei and Kampong Gua, Pahang, Peninsular Malaysia. *Courier Forschung. Senckenberg*, 182: 487-495.

Moh'd B.K. (1989) - Ar Rabba 1:50 000 geological map sheet. Geology Directorate, NRA, Amman.

Münster G. Graf zu (1841) - Beiträge zur Petrefacten-Kunde. IV.Beschreibung und Abbildung der in den Kalkmergelschichten von St. Cassian gefundenen Versteinerungen. Buchner'sche Buchhandlung, Bayreuth, 152 pp.

Nakazawa K. (1977) - On *Claraia* of Kashmir and India. *J. Palaeontol. Soc. India,* 20: 191-203.

Neri C. & Posenato R. (1985) - New biostratigraphical data on uppermost Werfen Formation of western Dolomites (Trento Italy). *Geol. Paläont. Mitt. Innsbruck,* 14(3): 87-107.

Newell N.D. & Boyd D. W. (1995) - Pectinoid bivalves of the Permian-Triassic crisis. *Bull. Am. Mus. Nat. Hist.,* 227: 1-95.

Nicora A. & Perri M.C. (1999) - The P/T Boundary in the Tesero section, western Dolomites (Trento). 3.3 Bio-and chronostratigraphy: conodonts: 97-100. In: Cassinis G. et al. (Eds) - Stratigraphy and facies of the Permian deposits between eastern Lombardy and the western Dolomites. Field Trip Guidebook - 23-25 September, 1999. International field conference on "The continental Permian of the Southern Alps and Sardinia (Italy), Regional reports and general correlations" 15-25 September 1999, Brescia, Pavia, Italy.

Ogilvie Gordon M. (1927) - Das Grödner - Fassa und Enneberggebiet in den Südtiroler Dolomiten. Stratigraphie-Tektonik. *Abh. Geol. Bund., Wien,* 24(1): 1-376.

Orchard M.J. (2007) - Conodont diversity and evolution through the latest Permian and Early Triassic upheavals. *Palaeogeogr., Palaeoclimatol., Palaeoecol.*, 252: 93-117.

Orchard M. J. & Krystyn L. (1998) - Conodonts of the lowermost Triassic of Spiti, and new zonation based on Neogondolella successions. *Riv. It. Paleontol. Strat.*, 104: 341-367.

Perri M.C. (1991) - Conodont biostratigraphy of the Werfen Formation (Lower Triassic), Southern Alps, Italy. *Boll. Soc. Paleontol. It.*, 30: 23-46.

Perri M.C. & Andraghetti M. (1987) - Permian–Triassic and Early Triassic conodonts from the Southern Alps, Italy, *Riv. It. Paleontol. Strat.*, 93: 291-328.

Perri M.C. & Farabegoli E. (2003) - Conodonts across the Permian-Triassic boundary in the Southern Alps. *Courier Forschung. Senckenberg*, 245: 281-313.

Perri M.C., Molloy P.D. & Talent J.A. (2004) - Earliest Triassic conodonts from Chitral, northernmost Pakistan. *Riv. It. Paleontol. Strat.*,110: 467-478.

Posenato R. (1992) - *Tirolites* (Ammonoidea) from the Dolomites, Bakony and Dalmatia: Taxonomy and biostratigraphy. *Eclogae Geol. Helv.,* 85(3): 893-929.

Posenato R., Sciunnach D. & Garzanti E. (1996) - First report of *Claraia* in the Servino Formation (Lower Triassic) of the western Orobic Alps, Italy. *Riv. It. Paleontol. Strat.*, 102(2): 201-210.

Posenato R. (2008a) - Global correlations of mid Early Triassic events: the Induan/ Olenekian boundary in the Dolomites (Italy). *Earth-Sci. Rev.,* 91: 93-105.

Posenato R. (2008b) - Patterns of bivalve biodiversity from Early to Middle Triassic in the Southern Alps (Italy): regional vs. global events. *Palaeogeogr., Palaeoclimatol., Palaeoecol.*, 261: 145-159.

Powell J.H. (1989) - Stratigraphy and sedimentation of the Phanerozoic rocks in central and south Jordan: Part A, Ram and Khreim Groups. Geological Mapping Division Bulletin, 11A. Geology Directorate, NRA, Amman.

Powell J.H. & Moh'd B. K. (1993) - Structure and sedimentation of Permo-Triassic and Triassic rocks exposed in small-scale horsts and grabens of pre-Cretaceous age; Dead Sea margin, Jordan. *J. African Earth Sci.* (and the Middle East), 17: 131-143.

Powell J.H, Abed A. M. & Le Nindre Y-M. (2014) - Cambrian stratigraphy of Jordan, *GeoArabia*, 19: 134-81.

Powell J.H., Stephenson M.H., Nicora A., Rettori R., Borlenghi L.M. & Perri M.C. (2016) - The Permian-Triassic Boundary, Dead Sea, Jordan: transitional alluvial to marine depositional sequences and biostratigraphy. *Riv. It. Paleontol. Strat.*, 122: 23-40.

Purnell M.A. & Donaghue P.C.J. (1998) - Skeletal architecture, homologies and taphonomy of ozarkodinid conodonts.

Palaeontology, 4: 57-102.

Purnell M.A., Donoghue P.C.J. & Aldridge R.J. (2000) - Orientation and anatomical notation in conodonts. *J. Paleontol.*, 74(1): 113-122.

Rettori R. (1995) - Foraminiferi del Trias inferiore e medio della Tetide: Revisione tassonomica, stratigrafia ed interpretazione filogenetica. *Publ. Dép. Géol. et Paléontol., Univ. Genève,* 18: 1-147.

Rexroad C.B. (1957) - Conodonts from the Chester Series in the type area of southwestern Illinois. *Illinois Geol. Surv. Rept. Invest.*, 209: 43 pp.

Rexroad C. B. & Furnish W. M. (1964) - Conodonts from the Pella Formation (Mississippian), south-central Iowa. *J. Paleont.*, 38: 667-676.

Schauroth C. (1857) - Die Schalthierreste der Lettenkohlenformation des Grossherzogthums Coburg. *Zeitschr. deutsch. Geol. Ges.,* 9: 85-148.

Scholze F., Abu Hamad A., Schneider J.W., Golubev V.K., Sennikov A.G., Voigt S. & Uhl D. (2017) - An enigmatic 'conchostracan' fauna in the eastern Dead Sea region of Jordan: First records of Rossolimnadiopsis Novozhilov from the Early Triassic Ma'in Formation. *Palaegeoogr., Palaeoclimatol., Palaeoecol.*, 466: 314-325.

Sharland P.R., Archer R., Casey D.M., Davies R.B., Hall S.H., Heward A.P., Horbury A.D. & Simmons M.D. (2001) - Arabian Plate Sequence Stratigraphy. *GeoArabia* Special Publication 2, Gulf PetroLink, Bahrain, 371 p., with 3 charts.

Sharland P.R., Casey D.M., Davies R.B., Simmons M.D. & Sutcliffe O.E. (2004) - Arabian Plate Sequence Stratigraphy – revisions to SP2. *GeoArabia*, 9: 199-214.

Shawabakeh K. (1998) - The geology of the Ma'in area - map sheet no. (3155 III): Hashemite Kingdom of Jordan, Natural Resources Authority; Geology Directorate, *Geological Mapping Division Bulletin*, 40: 1-74.

Song H., Tong J. & Chen Z.Q. (2009) - Two episodes of foraminiferal extinction near the Permian-Triassic boundary at the Meishan section, South China. *Austral. J. Earth Sci.*, 56: 765-773.

Song H., Tong J., Wignall P.B., Luo M., Tian L., Song H., Huang Y. & Chu D. (2016) - Early Triassic disaster and opportunistic foraminifers in South China. *Geol. Mag.*, 153: 298-315.

Stampfli G.M. & Borel G. (2002) - A plate tectonic model for the Palaeozoic and Mesozoic constrained by dynamic plate boundaries and restored synthetic oceanic isochrones. *Earth Planet. Sci. Lett.*, 196: 17-33.

Staesche U. (1964) - Conodonten aus dem Skyth von Südtirol, *Neues Jahr. Geol. Paläontol., A* 119: 247-306.

Sweet W. C. (1981) - Family Ellisonidae Clark, 1972. In: Robinson R.A. (Ed.) - Treatise on Invertebrate Paleontology. Part W, Miscellanea, Supplement 2, Conodonta, W152–W154. Geological Society of America and the University of Kansas Press, Lawrence.

Sweet W.C. (1988) - The Conodonta: Morphology, Taxonomy, Paleoecology, and Evolutionary History of a Long-extinct Animal Phylum. Oxford Monographs on Geology and Geophysics, 10: 1-212. Clarendon Press, Oxford.

Stephenson M.H. & Powell J.H. (2013) - Palynology and alluvial architecture in the Permian Umm Irna Formation, Dead Sea, Jordan. *GeoArabia*, 18: 17-60.

Stephenson M.H. & Powell J.H. (2014) - Selected spores and pollen from the Permian Umm Irna Formation, Jordan, and their stratigraphic utility in the Middle East and North Africa. *Riv. It. Paleontol. Stratigr.*, 120: 145-156.

Tommasi A. (1895) - Contributo alla fauna del calcare bianco del Latemar e della Marmolada. *Atti Acc. Agiati, Rovereto,* 1(3): 77-83.

Ueno K., Miyahigashi A. & Martini R. (2018) - Taxonomic and nomenclatural justification for the Triassic meandrospiral foraminiferal genus *Citaella* Premoli Silva, 1964. *J. Foramin. Res.*, 48(1): 62-74.

Wetzel R. & Morton D.M. (1959) - Contribution à la Géologie de la Transjordanie. *Notes et Mémoires de la Moyen Orient, Muséum National d'Histoire Naturelle, Paris*, 7: 95-191.

Wignall P. (2001) - Large igneous provinces and mass extinctions. *Earth Sci. Rev.*, 53: 1-33.

Wittenburg P. von (1908) - Beiträge zur Kenntnis der Werfener Schichten Süd-tirols. *Geol. Palaeont. Abh.* 8: 251-289.

Yang B., Yuan D.-X., Henderson C. M. & Shen S.-Z. (2014) - *Parafurnishius*, an Induan (Lower Triassic) conodont new genus from northeastern Sichuan Province, southwest China and its evolutionary implications. *Palaeoworld,* 23: 263-275.

Youngquist W. & Miller A. K. (1949) - Conodonts from the Late Mississippian Pella beds of south-central Iowa. *J. Paleont.*, 23: 617-622.